Advanced Detector Technology

Luciano Musa - CERN

CERN-FERMILAB
HADRON COLLIDER PHYSICS
Summer School 2015

Lecture 1/3
CERN, 30 August 2017

Lecture 1

- Tracking detectors in HEP experiments
- Silicon trackers – a brief historical excursus
- Silicon properties – a brief reminder
- Silicon detectors – basic principles

This lecture makes use of material from the following authors

- *Mohsen Khakzad* (St FX University, Canada)
- *M. Krammer (CERN and IHEP Vienna, Austria), F. Hartmann (KIT, Germany)*
- *N. Wermes (Bonn University, Germany)*
- *P. Riedler (CERN), A. Kluge* (CERN)
- *D. Bortoletto* (Oxford University, UK)

Introduction

Tracking Detectors in HEP Experiments

Trackers – Key to Solve Complex Events

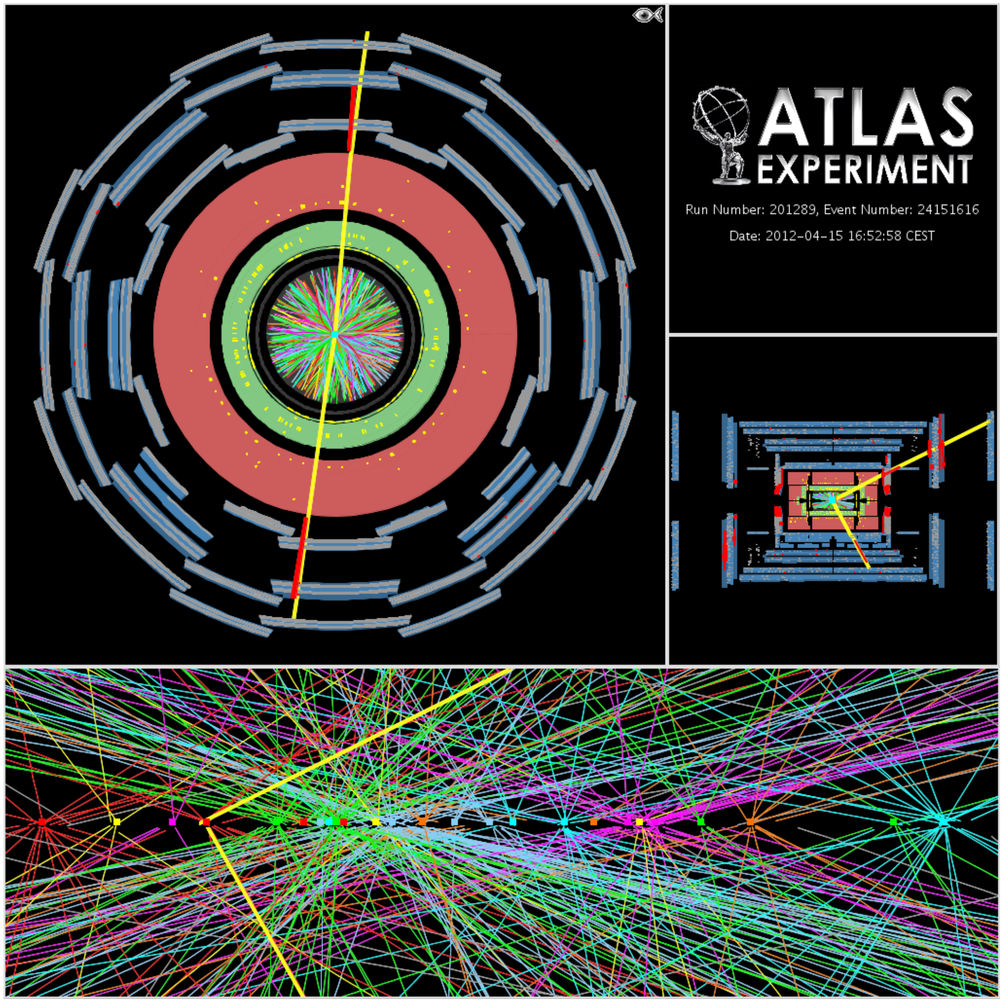

LHC pp collisions: a candidate Z boson event in the dimuon decay with 25 reconstructed vertices (ATLAS, April 2012)

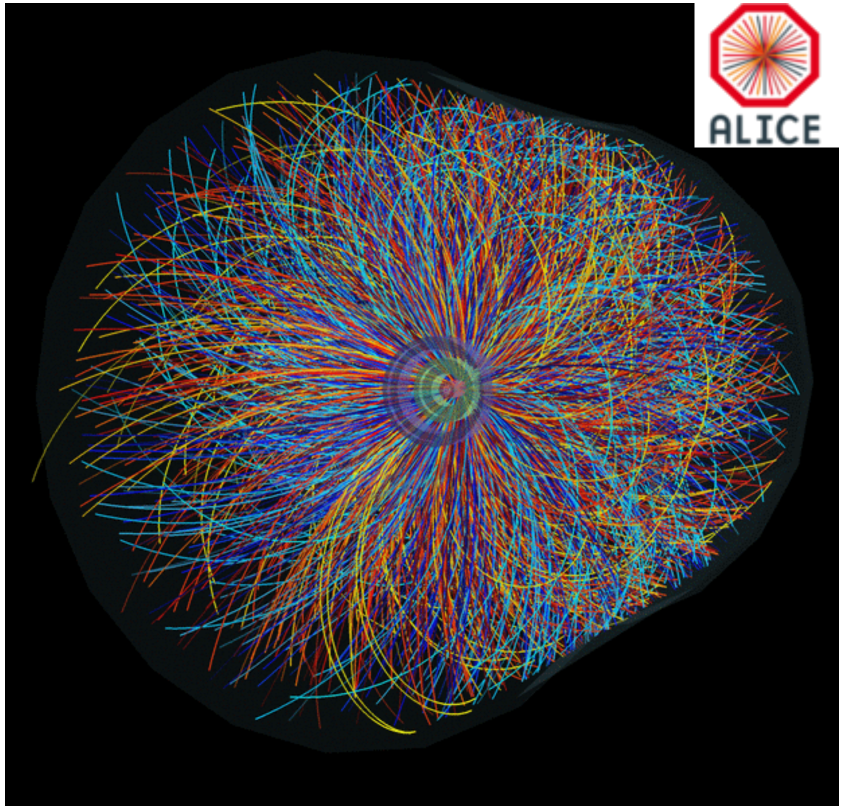

LHC Pb-Pb collision (ALICE, Sep 2011)

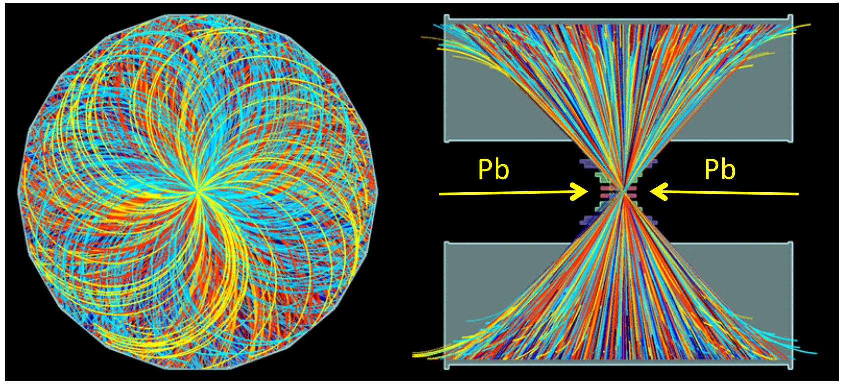

Introduction

Fixed Target Exp:

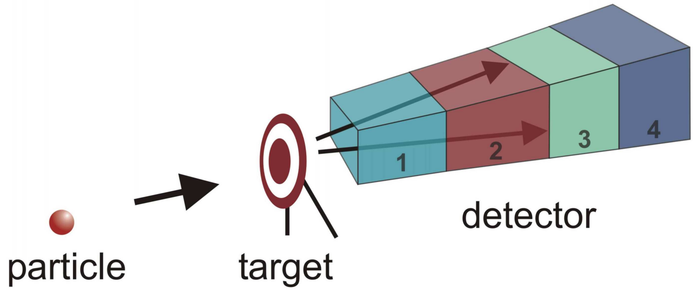

Collider Exp:

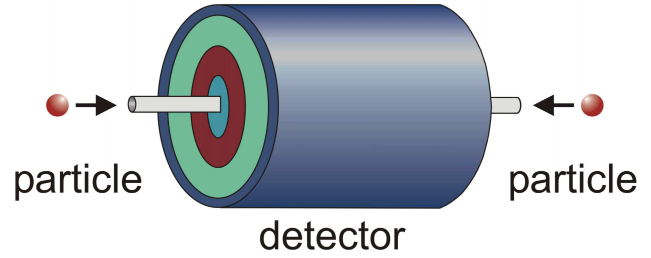

Interaction of particles in diff. detector components:

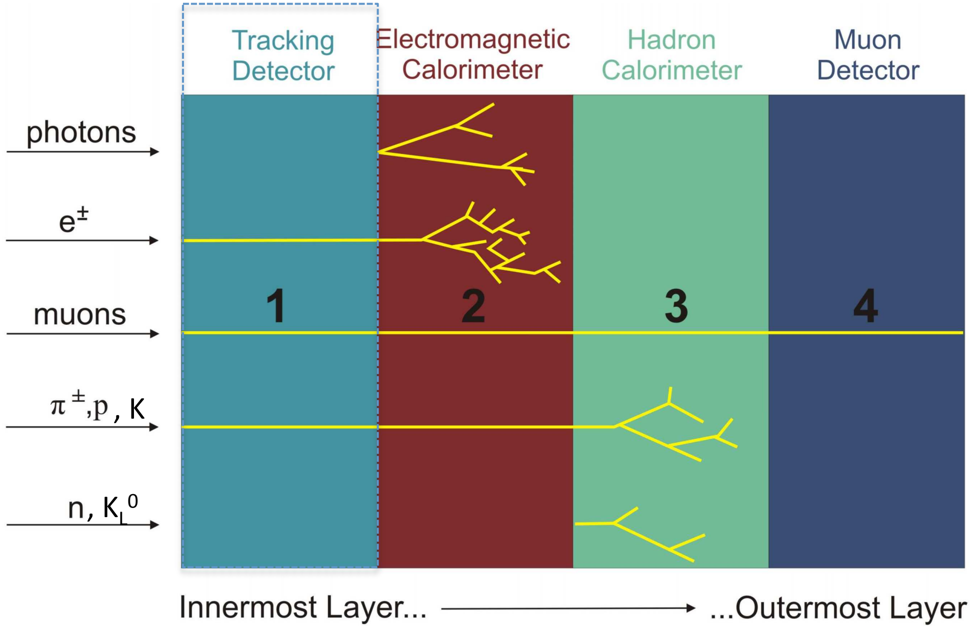

Traditional Particle Physics Experiment divided (simplified) in 4 main components

By the characteristic signatures particles leave in a detector

- particles can be either identified: e^-, e^+, μ^-, μ^+, γ
- or at least assigned to families: charged or neutral hadrons

Introduction – Tracking System

Tracking system measures the traces left by charged particles

Tracking + Magnetic Field: magnetic spectrometer ➔ sign and momentum

Photons may convert into electron-positron pair, which can be detected in the tracking system

Charged kaon decays may be detected in a high-resolution tracking system through their characteristic "kink" topology:

$$K^{\pm} \to \mu^{\pm}\nu_{\mu} \quad (64\%)$$
$$K^{\pm} \to \pi^{\pm}\pi^{0} \quad (21\%)$$

The kinematics of this kink topology allows separating *K* decays from the main source of background kinks from charged pion decays

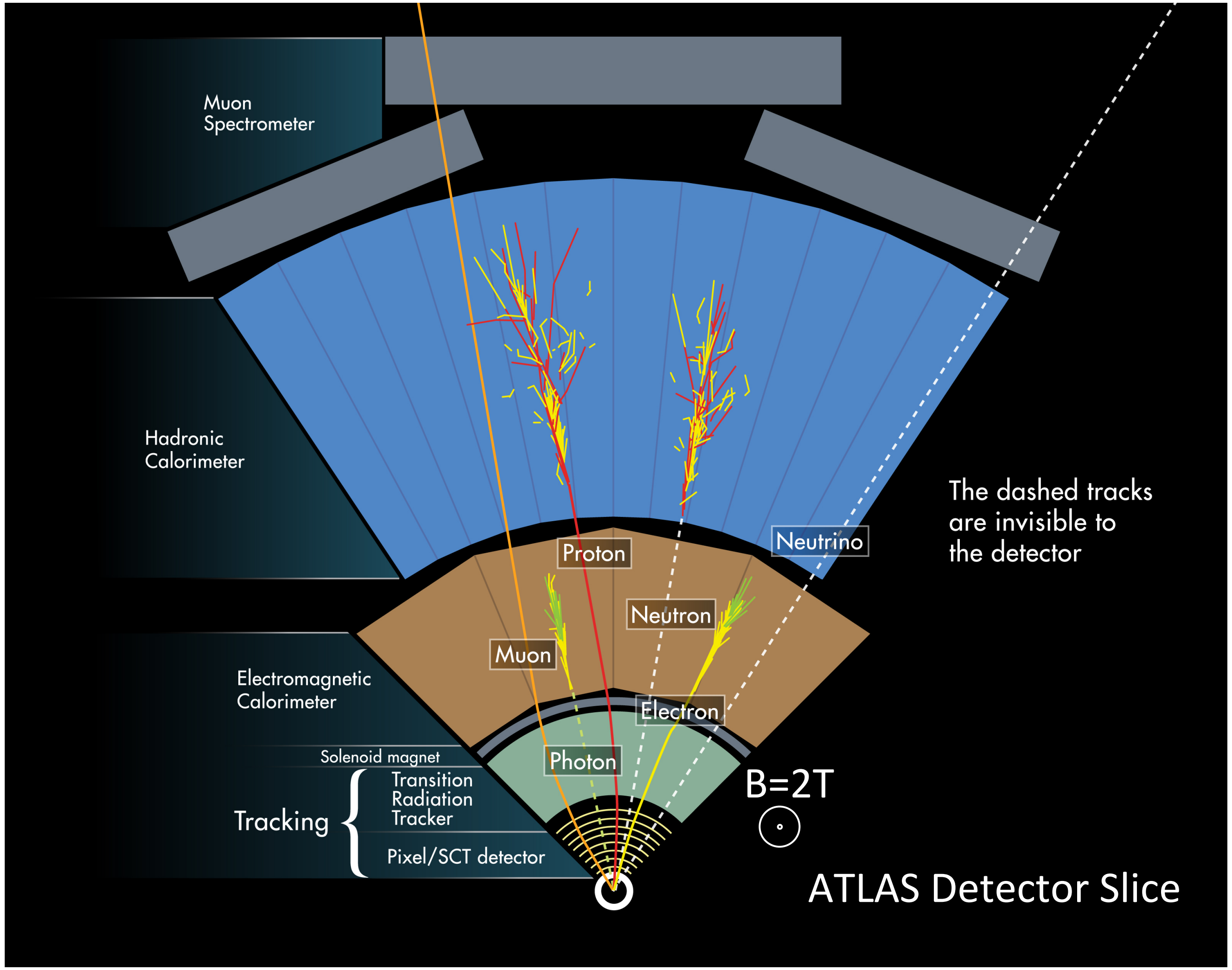

Momentum Measurement in a Magnetic Spectrometer

Almost all High Energy Physics (HEP) experiments with accelerators make use of magnetic spectrometers to determine the momentum of charged particles

If a particle with mass m_0 and charge **q** traverses a magnetic field **B** with velocity **v**

$$\frac{m\upsilon^2}{R} = q\upsilon B \qquad \boxed{R = \frac{m\upsilon}{qB}}$$

Lorentz force $\boxed{\frac{d\bar{p}}{dt} = \bar{F} = q\bar{\upsilon} \times \bar{B}}$

In case of homogeneous magnetic field the trajectory is given by an helix

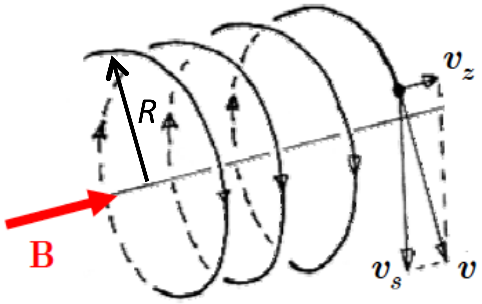

In experiments at hadronic colliders the emphasis is on the measurement of the transverse momentum p_T

$$\boxed{p_T[GeV/c] = 0.3B[T] \cdot R[m]}$$

Use layers of position sensitive detectors before and after or inside a magnetic field to measure the trajectory and determine the bending radius R

$$\boxed{\frac{\delta p}{p} = \frac{p}{0.3BL^2}\sigma \cdot \sqrt{C_N}}$$

The relative error on the momentum is:

- proportional to p
- inversely proportional to B
- inversely proportional to L^2
- proportional to the detector spatial resolution σ

BL^2 = bending power

Momentum Measurement in a Magnetic Spectrometer

Assume N+1 detection layers, placed at x_0, x_1, x_N, measuring the y coordinate all with the same resolution

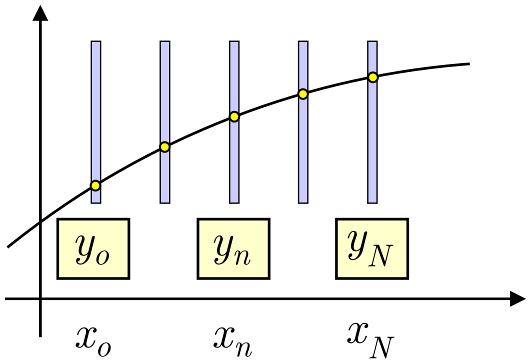

$$\frac{\delta p}{p} = \frac{p}{0.3BL^2}\sigma \cdot \sqrt{C_N}$$

true if multiple-scattering is neglected

$$C_N = \frac{720N^3}{(N-1)(N+1)(N+2)(N+3)}$$

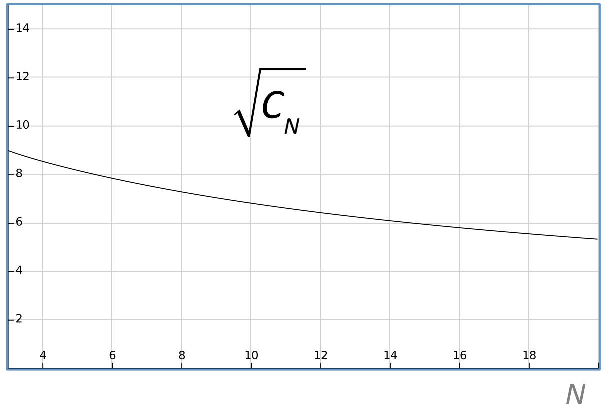

Weak dependence on N!!

Good momentum resolution requires

- Good spatial resolution
- Strong B field
- Long track path length (lever of arm)

Momentum resolution gets worse at large p!!

Magnetic Spectrometers

Two main configurations

Solenoidal field Central Barrel Spectrometer

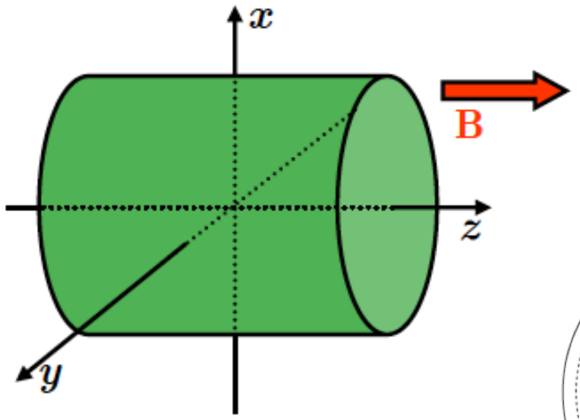

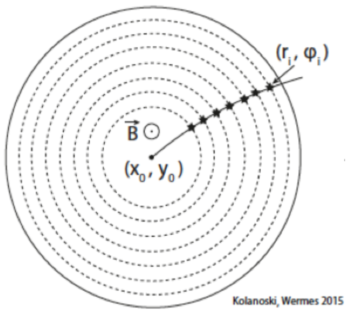

Cylindrical symmetry

- deflection in x-y (r-ϕ) plane
- Tracking detectors in cylindrical shells along r
- Measurment of curved tracks in r-ϕ plane (bending plane) at fixed values of r

Dipole field Forward Spectrometers

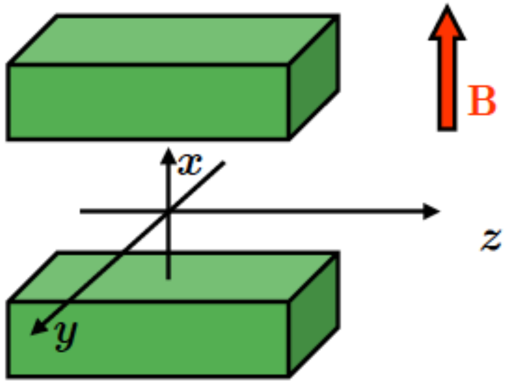

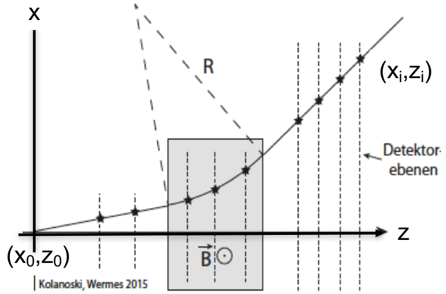

Rectangular symmetry

- deflection in y-z plane
- Tracking detectors arranged in parallel planes along z
- Measurment of curved tracks in y-z plane at fixed values of z
- Bending from difference of the slopes before and after B

Solenoid: CMS=4T, ATLAS=2T, ALICE=0.5T Dipole: LHCb=4Tm

LHCb – A Foward Spectrometer

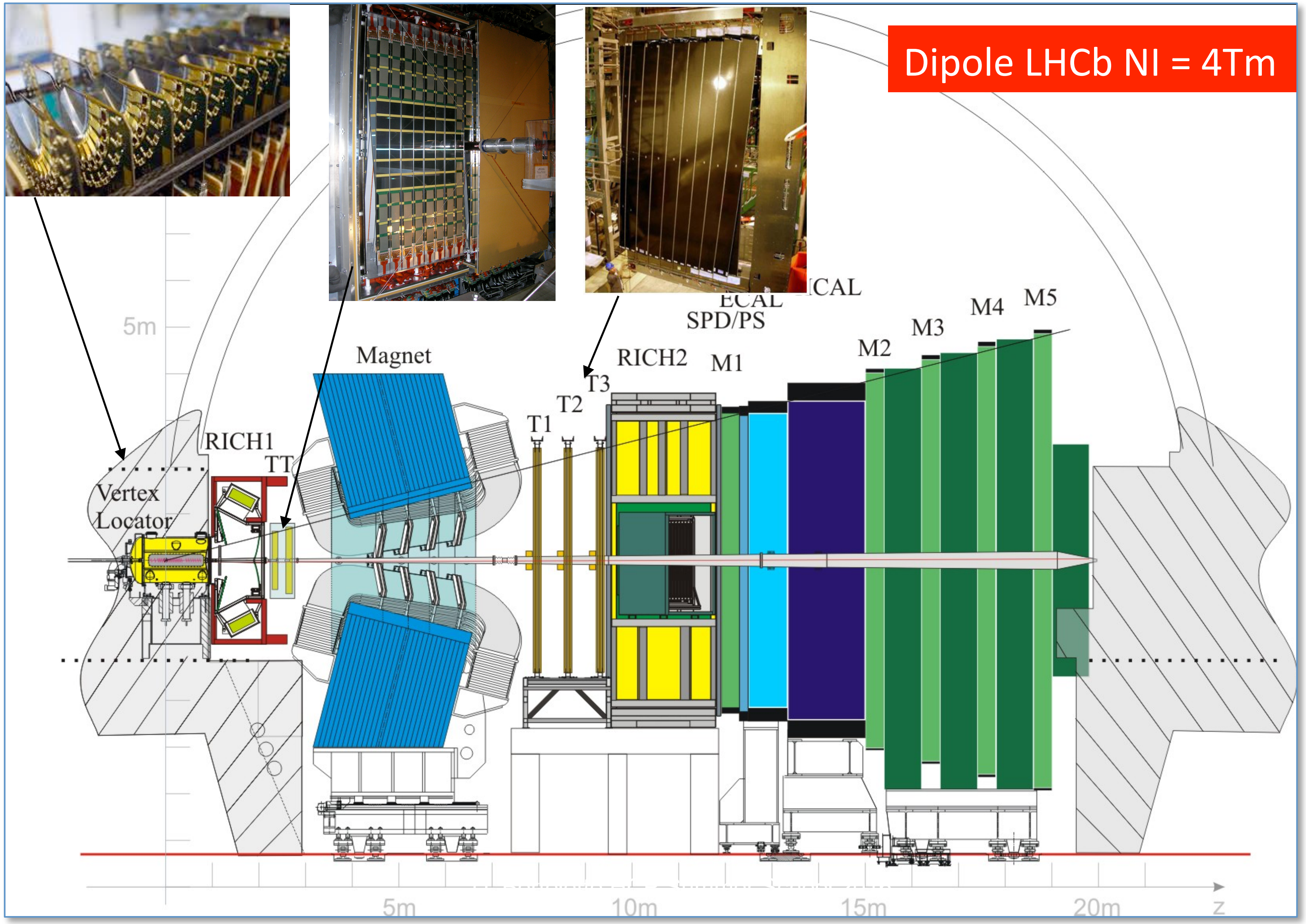

Magnetic Spectrometers

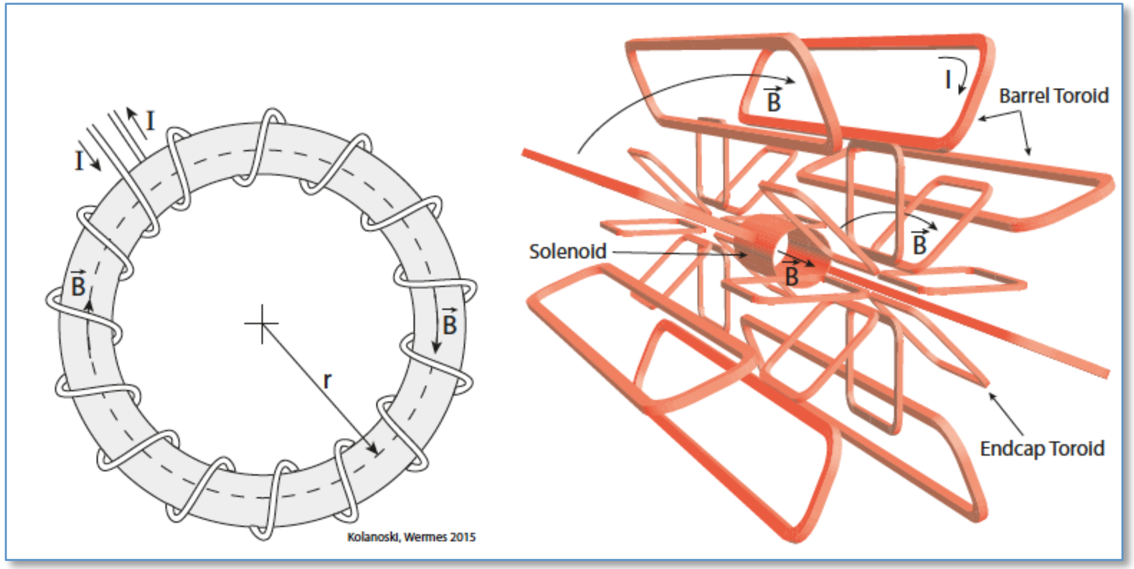

TOROID ATLAS 0.5T
Azimuthal symmetry

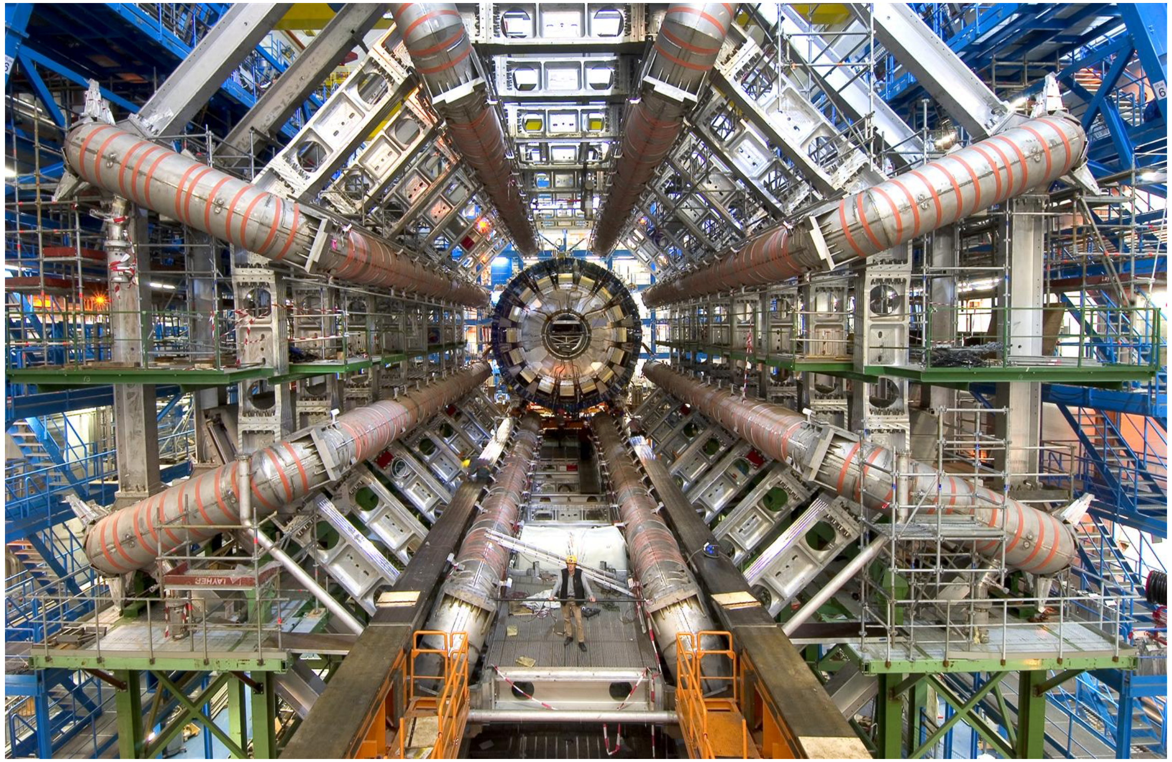

Azimuthal symmetry

- deflection in (r-z) plane
- Tracking detectors in cylindrical shells along r
- Measurment of curved tracks in r-z plane at fixed values of r

Multiple Scattering

Particles moving trough the detector material suffer innumerable EM collisions which alter the trajectory in a random fashion (stochastic process)

Statistical (quite complex) analysis of multiple coulomb collisions (Rutherford scattering at the nuclei of the detector material), gives:

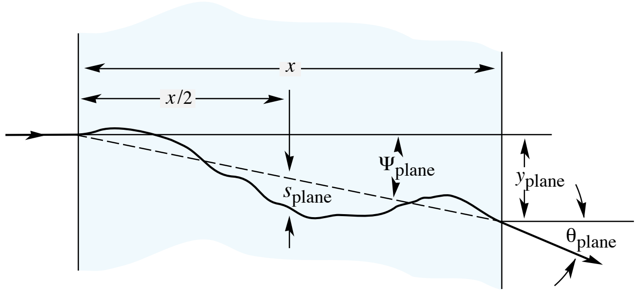

$$P(\theta_p) = \frac{1}{\sqrt{2\pi\langle\theta_p^2\rangle}} \exp\left[-\frac{1}{2\langle\theta_p^2\rangle}\theta_p^2\right]$$

Probability that a particle is deflected by an angle θ_p after travelling a distance x in the material is given by a (almost) Gaussian distribution with sigma of:

$$\langle\theta_p\rangle = \frac{0.0136}{\beta cp[GeV/c]} z_{particle} \sqrt{\frac{x}{X_0}} \cdot \left(1 + 0.038 \ln \frac{x}{X_0}\right)$$

High tracking resolution ⇨ less scattering

Spatial resolution ⇨ $\sigma \approx \frac{L}{N}\langle\theta_p\rangle = \frac{L}{N}\frac{0.0136}{p\beta}\sqrt{\frac{x}{X_0}}$

- Small x, i.e very thin detectors
- Large radiation length X_0 – i.e. low Z and low density materials (Be, C, Al, …)

Note: Lateral displacement ε_p displacement is proportional to the thickness of the detector: usually can be neglected for thin detectors (for 300 μm silicon $\varepsilon_p \approx 0.01$ μm)

Central Trackers at the LHC Experiments

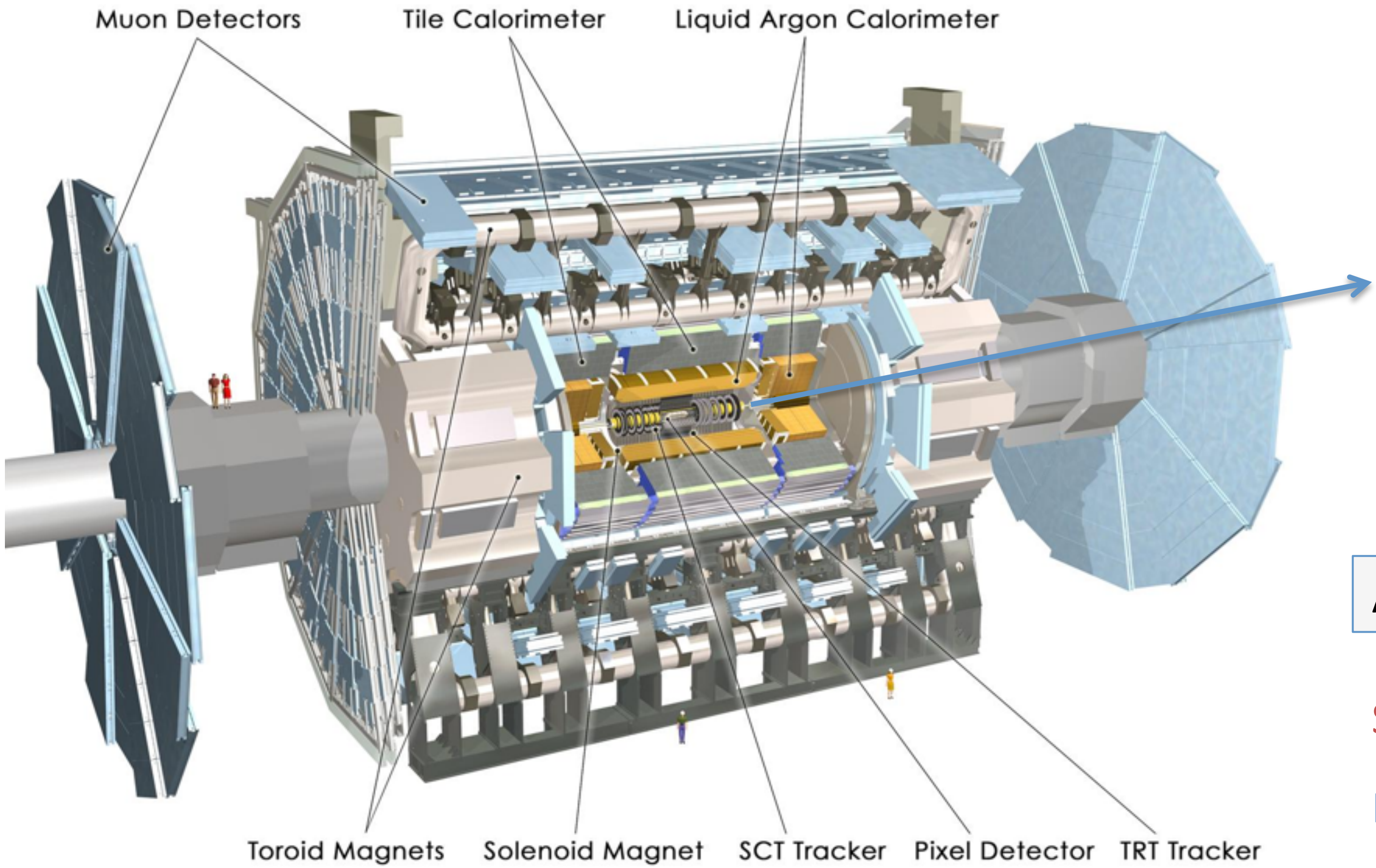

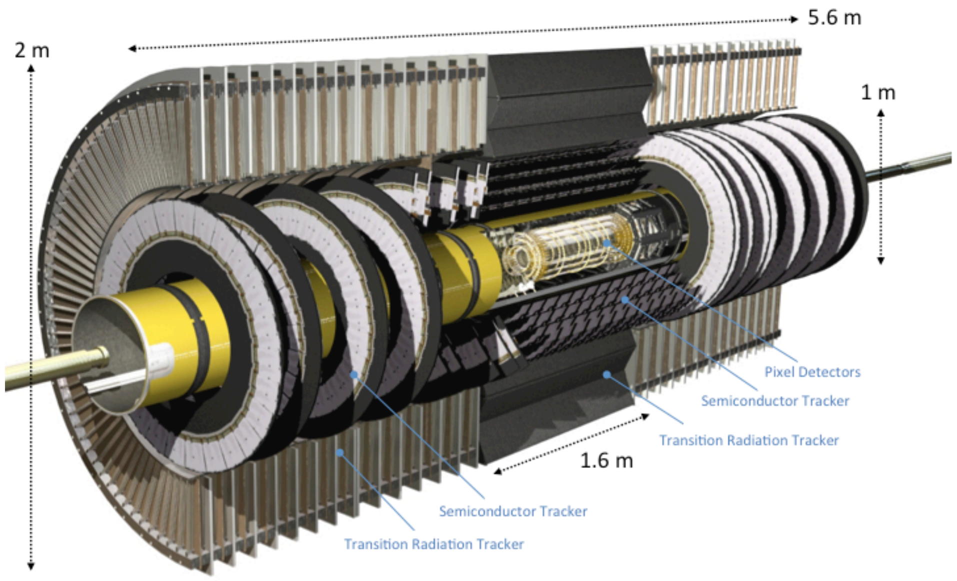

ATLAS Tracker

Si-pixel, Si strip, TRT (gas, transition radiation)

Phase-I upgrade: one more Si-pixel layer (IBL)

Phase-II upgrade: Si pixel + Si Strip (entirely new)

≈ 200 m^2 silicon strips

Central Trackers at the LHC Experiments

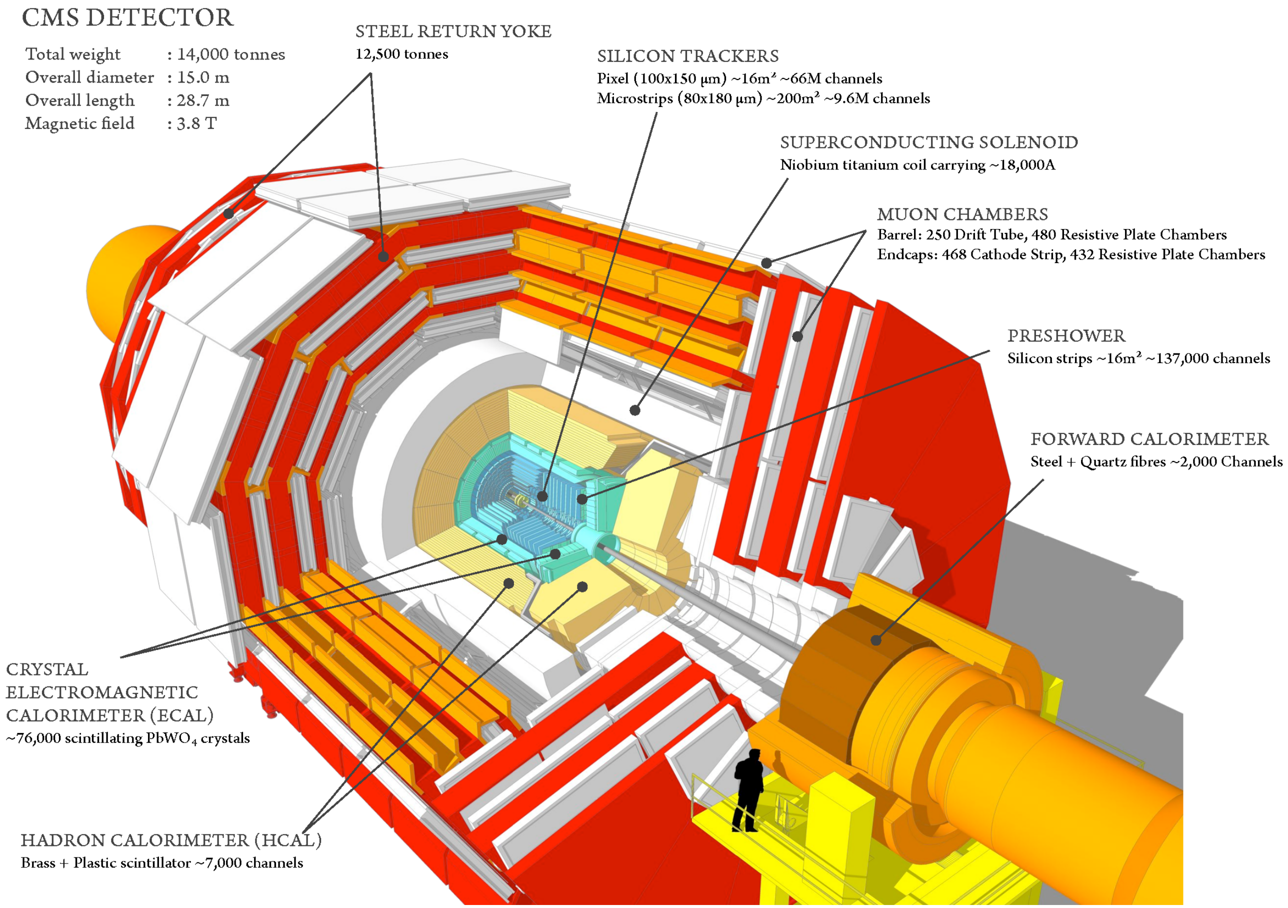

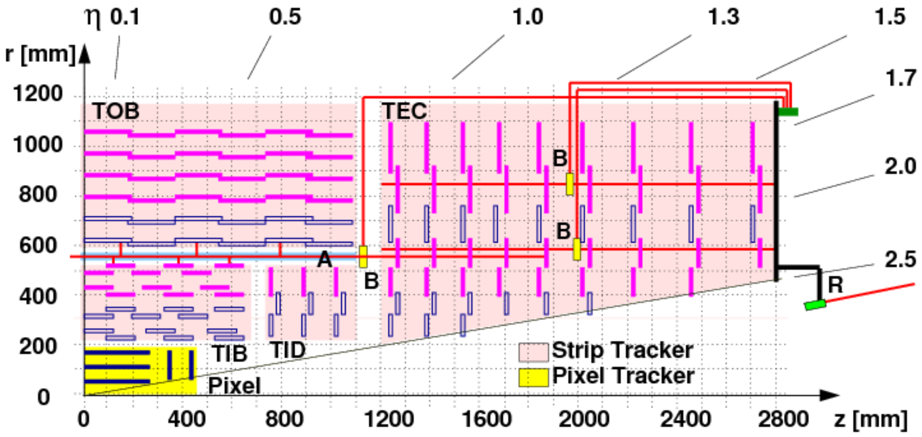

CMS Tracker

Si-pixel, Si strip ➡ **All silicon**

Phase-I upgrade: replacement of Si-pixel

Phase-II upgrade: Si pixel + Si Strip (entirely new)

≈ 200 m^2 silicon strips

Central Trackers at the LHC Experiments

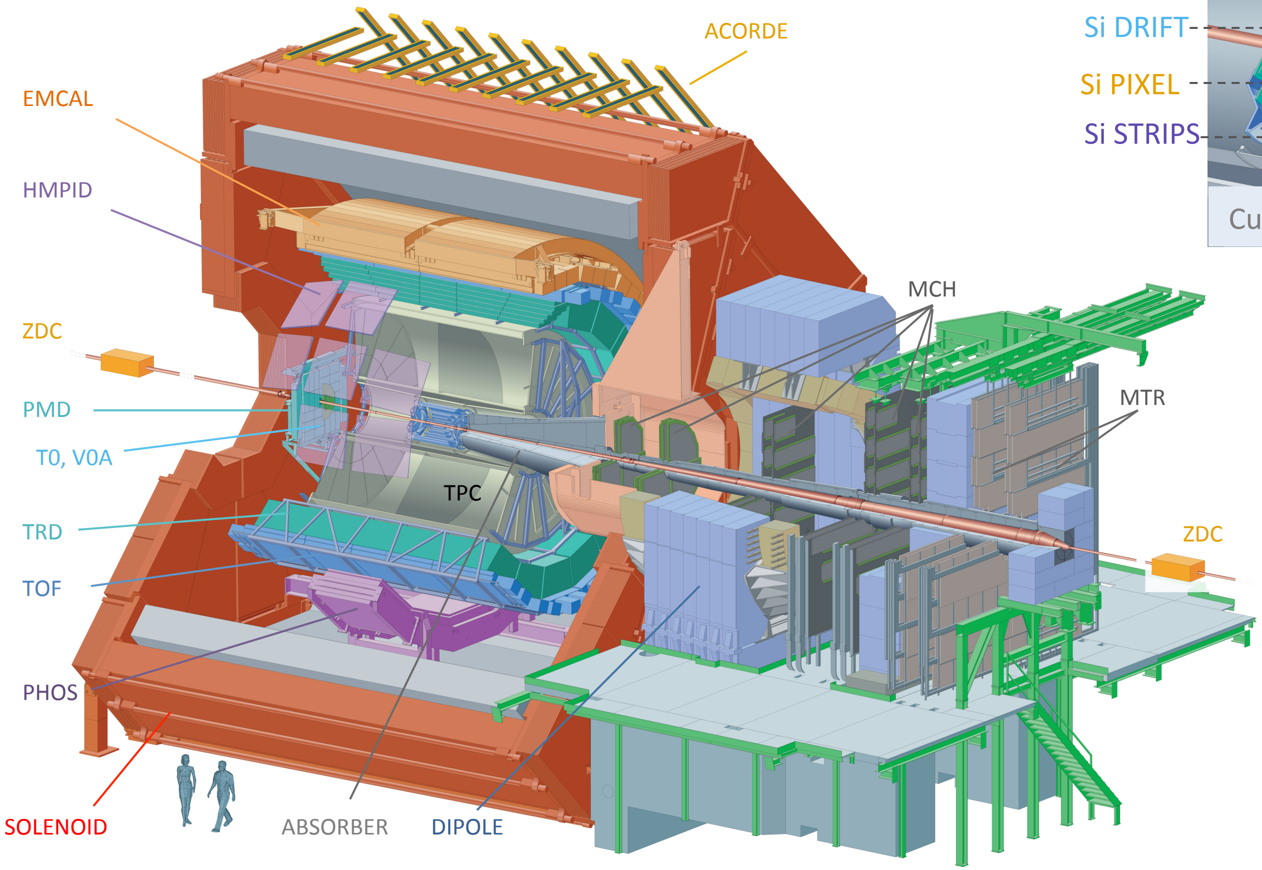

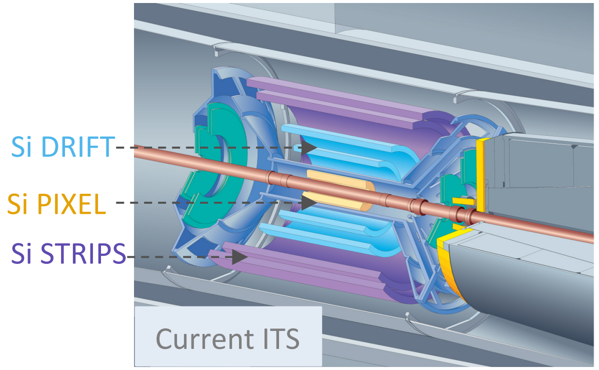

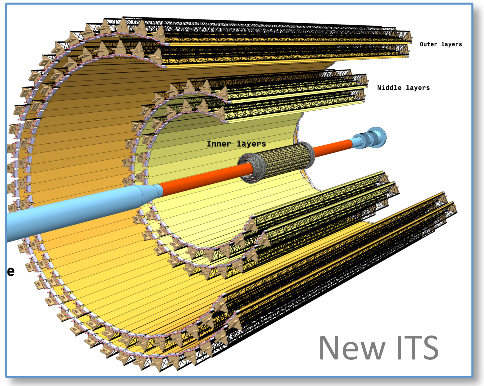

ALICE Tracker

Si pixel, Si drift, Si strip, TPC (gas), TRD (gas, trans. rad.)

Phase-I upgrade: MAPS + TPC & TRD (new readout)

10 m^2 silicon pixels

Central Trackers at the LHC Experiments

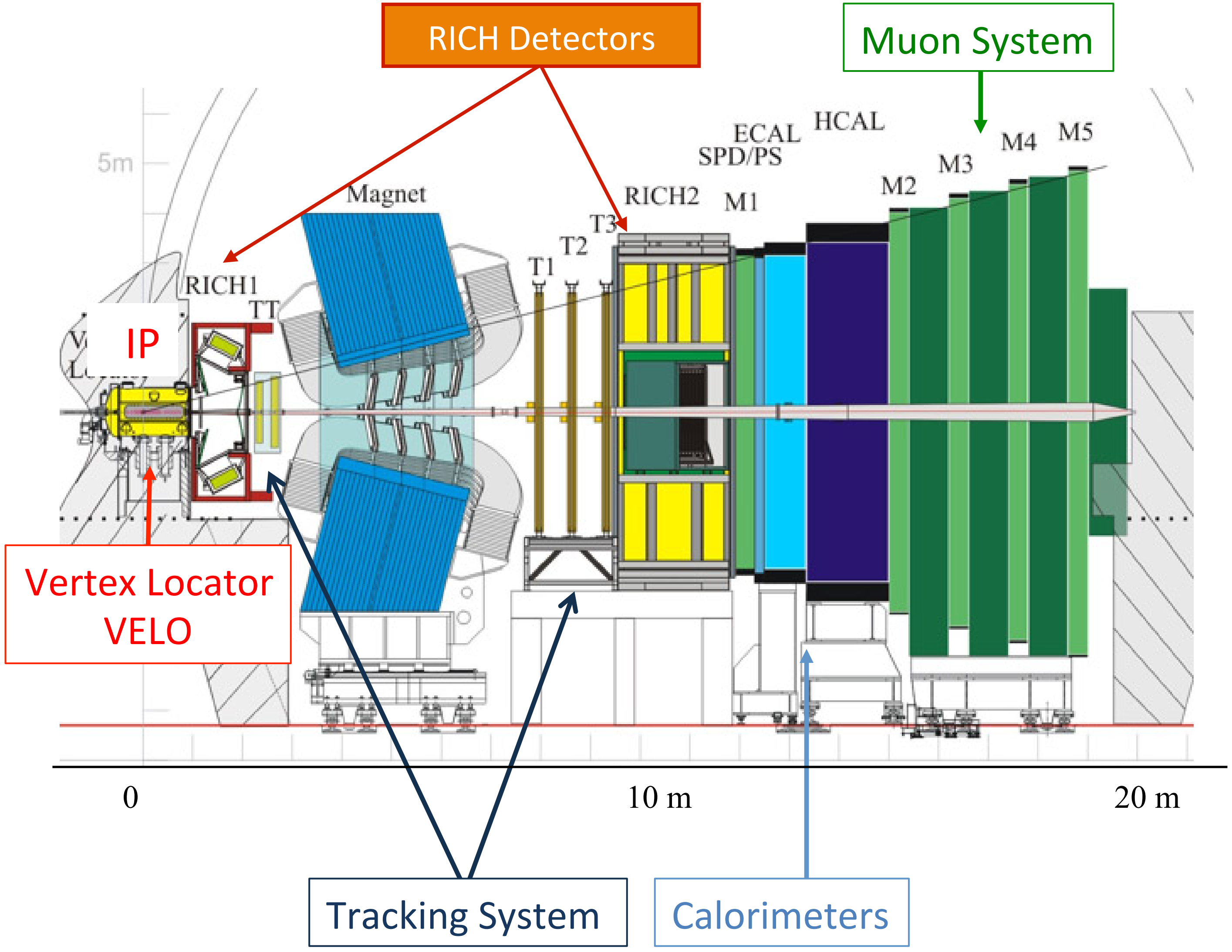

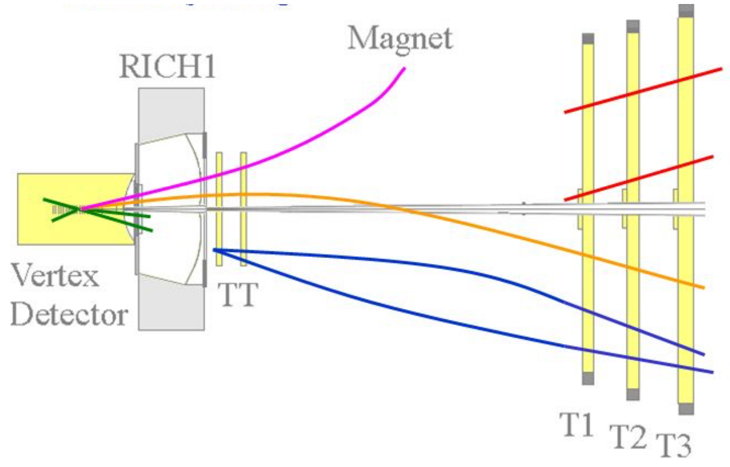

LHCb Tracker

Si strips (VELO), silicon+straw tubes

Phase-I upgrade: Si pixel, scintillating fibers

Pixels to cope with higher particle rates

Silicon Trackers

A Brief Historical Excursus

The Rise of Silicon Detectors in HEP

Towards end of 1970's: intensive R&D on devices which could measure short-lived particles ($\leq$ ps)

R&D at CERN(A) and Pisa(B) demonstrated that strip detectors (100-200μm pitch):

- exhibit high detection efficiency (>99%), good spatial resolution (~20μm) and good stability
- allow precise vertex reconstruction

However the technology for the fabrication of these devises was very tricky, thus limiting their availability

1980 – fabrication of silicon detectors using standard IC planar process (PIN diode ➔ μstrip detector)

J. Kemmer, et al., *"Development of 10-micrometer resolution silicon counters for charm signature observation with the ACCMOR spectrometer", Proceedings of Silicon Detectors for High Energy Physics, Nucl. Instr. and Meth. 169 (1980) 499.*

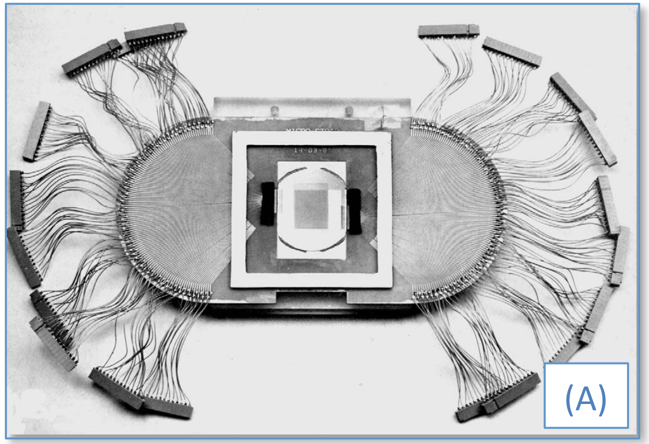
(A)

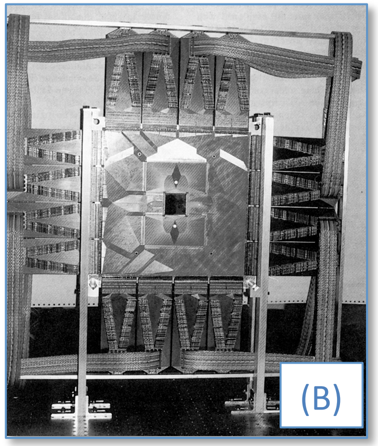
(B)

First use of silicon strips detectors by NA11(CERN SPS) and E706 (FNAL)

(A) NA11 (1981): 6 planes (24 x 36mm^2): resistivity 2-3 kΩcm, thickness 280μm, pitch 20μm

(B) E706 (1982): 4 planes (3x3 cm^2) + 2 planes (5x5cm^2)

Erik Heine, Joseph Kemmer and Gherard Lutz: 2017 EPS prize for "Outstanding Contributions to HEP" (pioneering the development of silicon μstrip)

The Rise of Silicon Detectors in HEP

The next step forward came with the advent of the VLSI technology that allowed coupling ASIC amplifier chips directly to the detectors

1990s - LEP, first silicon vertex detectors were installed in DELPHI and ALEPH experiments, then OPAL and L3

1989 - first DELPHI vertex detector, consisting of two layers of single-sided strip detectors

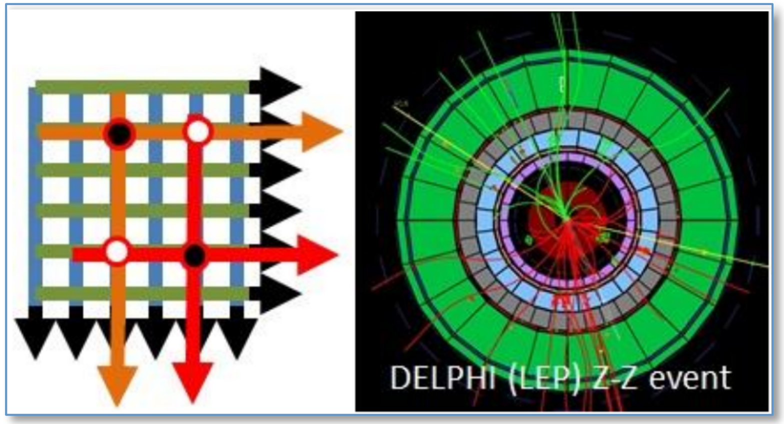

Projective geometry ➔ ambiguity at high multiplicities (high occupancy)

This started to become apparent already at DELPHI:

- High number of ambiguities ➔ reconstruction efficiency suffered a lot, especially in the forward direction

Not usable close to IP in hadron colliders (LHC) or HI experiments at SPS

Another problem at (very) high particle load ➔ degradation of the sensor by the high radiation dose

This implies starting with a very large signal-to-noise ratio, which can only be obtained with detector with small capacitance

The Inception of Silicon Pixel Detectors

"The silicon micropattern detector: a dream?"

E.H.M Heijine, P. Jarron, A. Olsen and N. Redaelli , *Nucl. Instrum. Meth. A 273 (1988) 615*

"Development of silicon micropattern detectors"

CERN RD19 collaboration, *Nucl. Instrum. Meth. A 348 (1994) 399*

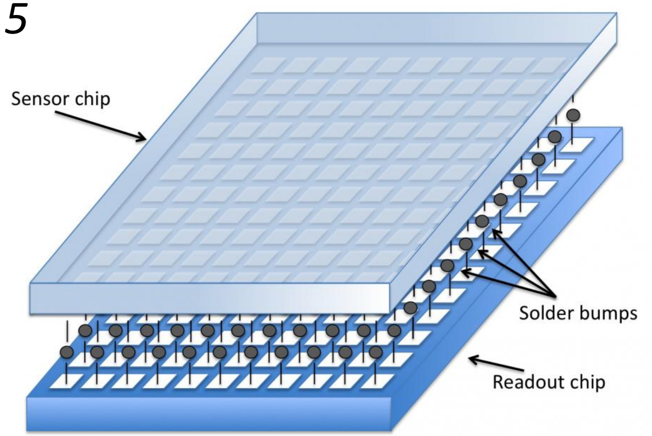

Hybrid pixel detector

1995 – First Hybrid Pixel detector installed in WA97 (CERN, Omega facility)

1996/97 – First Collider Hybrid Pixel Detector installed in DELPHI (CERN, LEP)

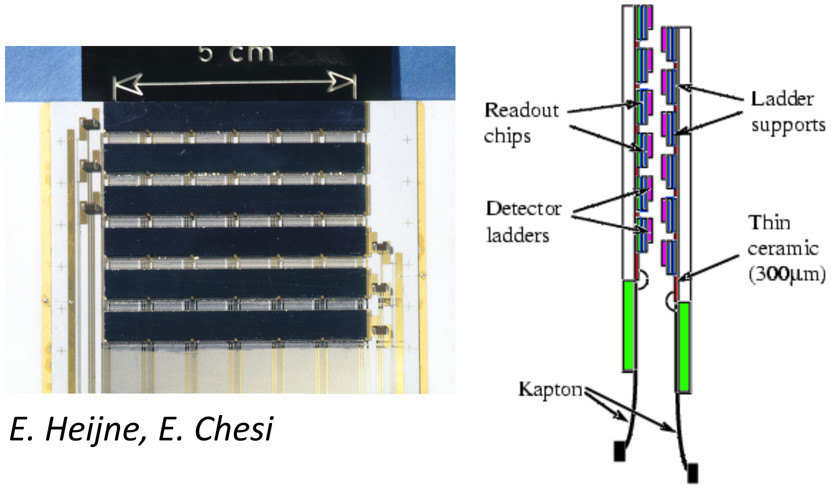

E. Heijne, E. Chesi

Work carried out by RD19 for WA97 and NA57/CERN

CERN – WA97 Experiment (1995)

- 5 x 5 cm^2 area
- 7 detector planes
- ~0.5 M pixels
- Pixel size 75 x 500 μm^2
- 1 kHz trigger rate
- Omega2 chip

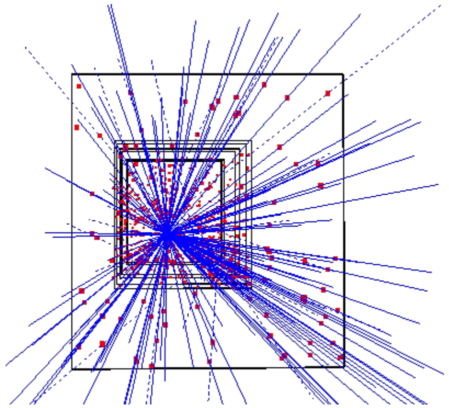
No-field, Pb-Pb, 153 reconstructed tracks

Pixel Detectors at the LHC Trackers

10 years after the first use in WA97… silicon detectors at the heart of the LHC Experiments

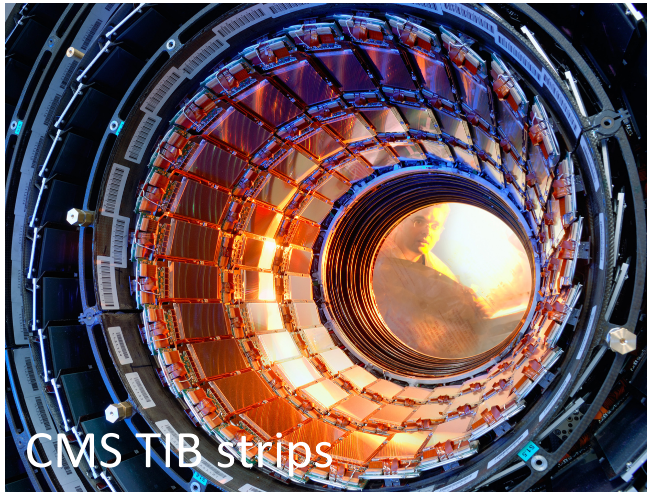

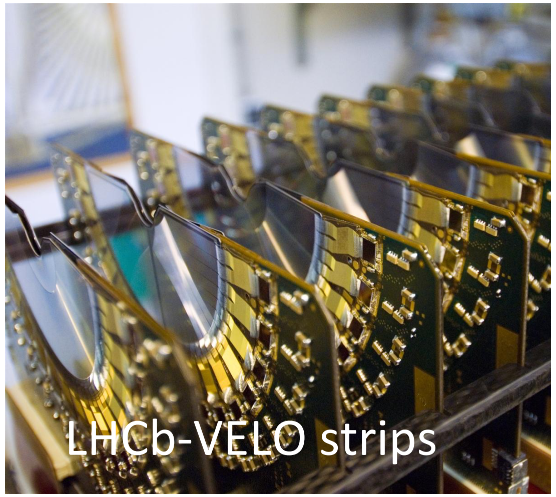

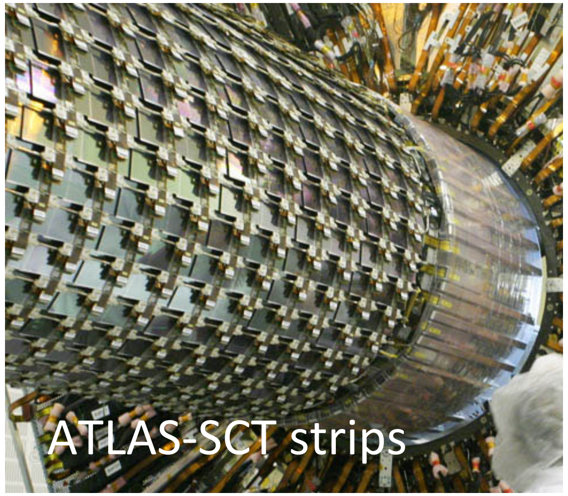

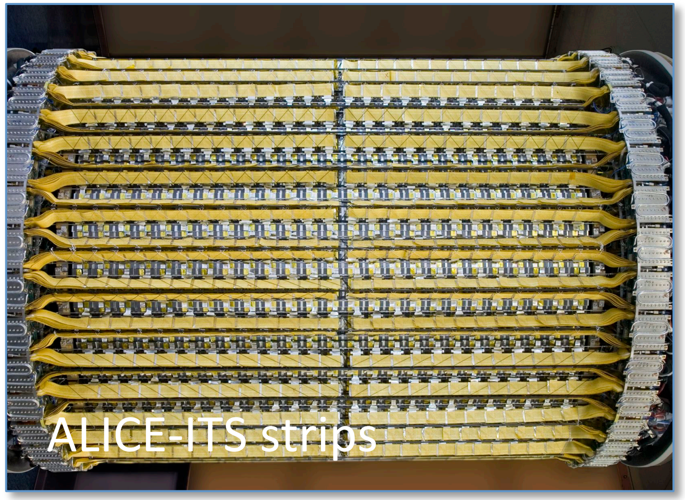

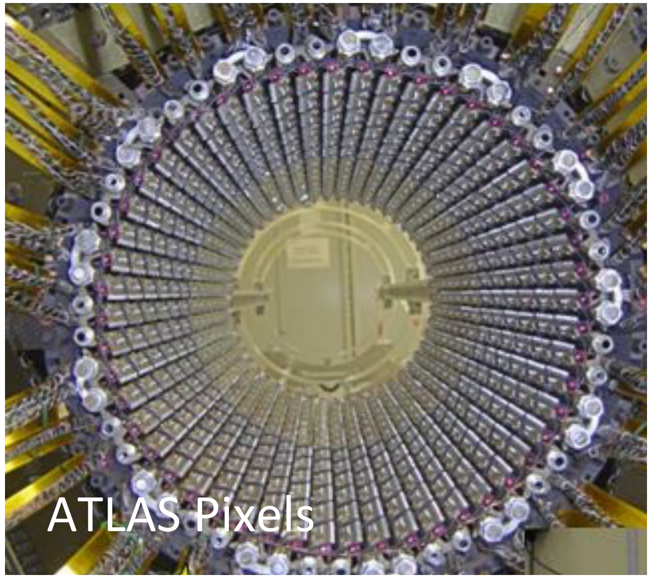

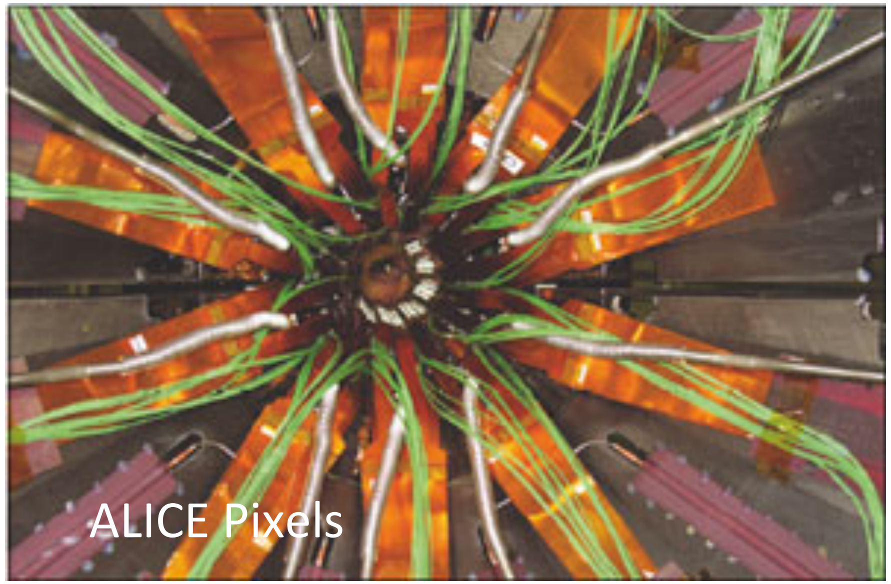

Beyond Hybrid Pixel Detectors …

Hybrid Pixel Detector

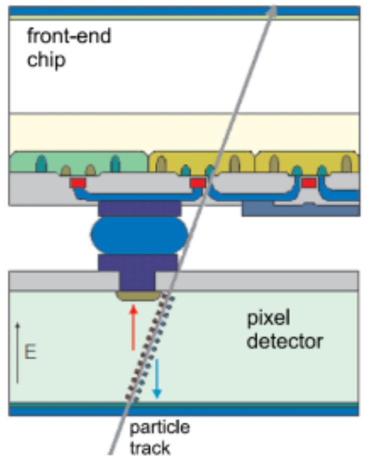

Monolithic Pixel Detector

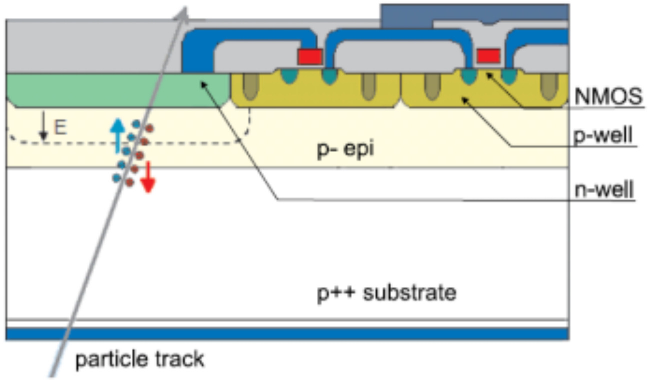

Since the very beginning of pixel development (RD 19):

dream to integrate sensor and readout electronics in one chip

Motivation to reduce: cost, power, material budget, assembly and integration complexity

Several major obstacles to overcome for CMOS MAPS:

- CMOS generally not available on high resistivity silicon (needed as bulk material for the sensor) ✔
- Full CMOS circuitry not possible within the pixel area (only one type of transistor ➔ slow readout) ✔

Beyond Hybrid Pixel Detectors - Monolithic Pixel Detectors

Owing to the industrial development of CMOS imaging sensors and the intensive R&D work (IPHC, RAL, CERN)

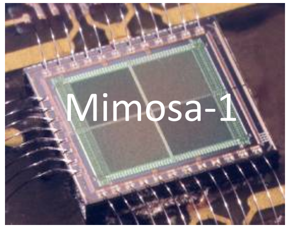

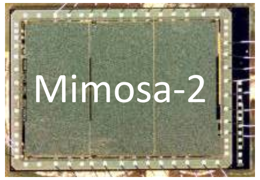

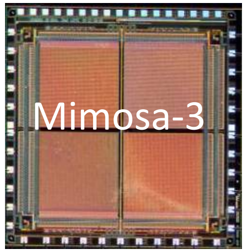

. . .

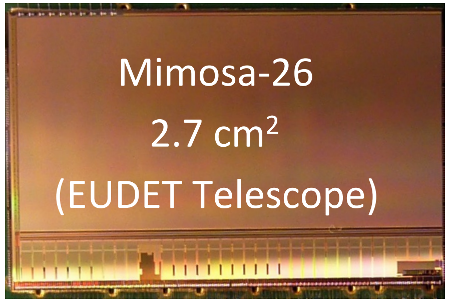

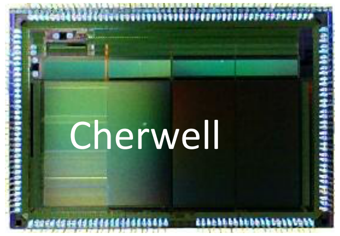

… several HI experiments have selected CMOS pixel sensors for their inner trackers and intensive R&D for ATLAS

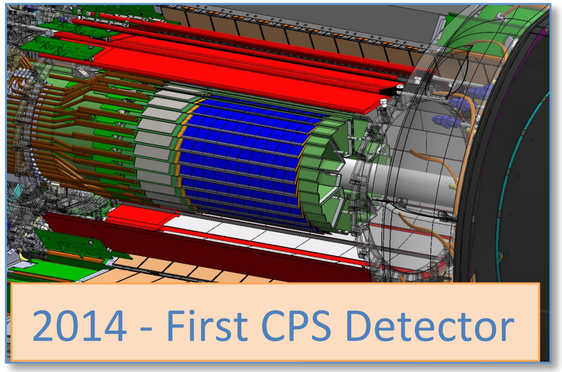

STAR HFT
0.16 m^2 – 356 M pixels

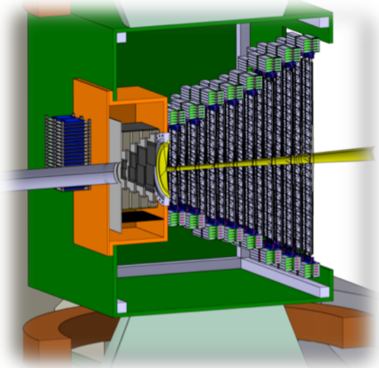

CBM MVD
0.08 m^2 – 146 M pixel

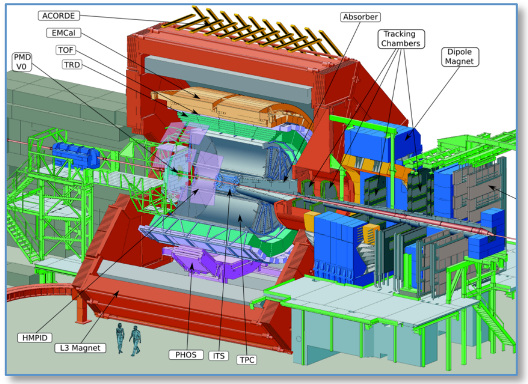

ALICE ITS Upgrade (and MFT)
10 m^2 – 12 G pixel

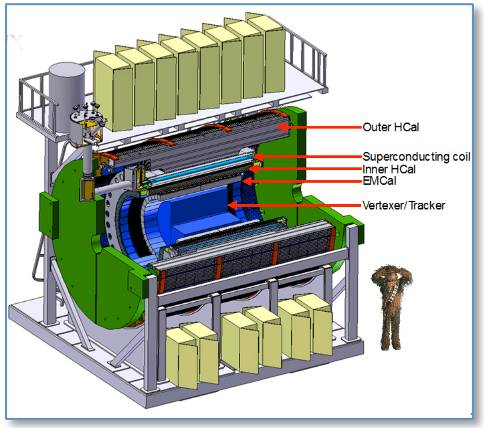

sPHENIX
0.2 m^2 – 251 M pixel

…

Silicon Properties

A Brief Reminder

Silicon CMOS Industry

Monocrystalline silicon

main semiconductor used for the fabrication of Integrated Circuits

Monocrystalline, high purity single crystals (Czochralski)

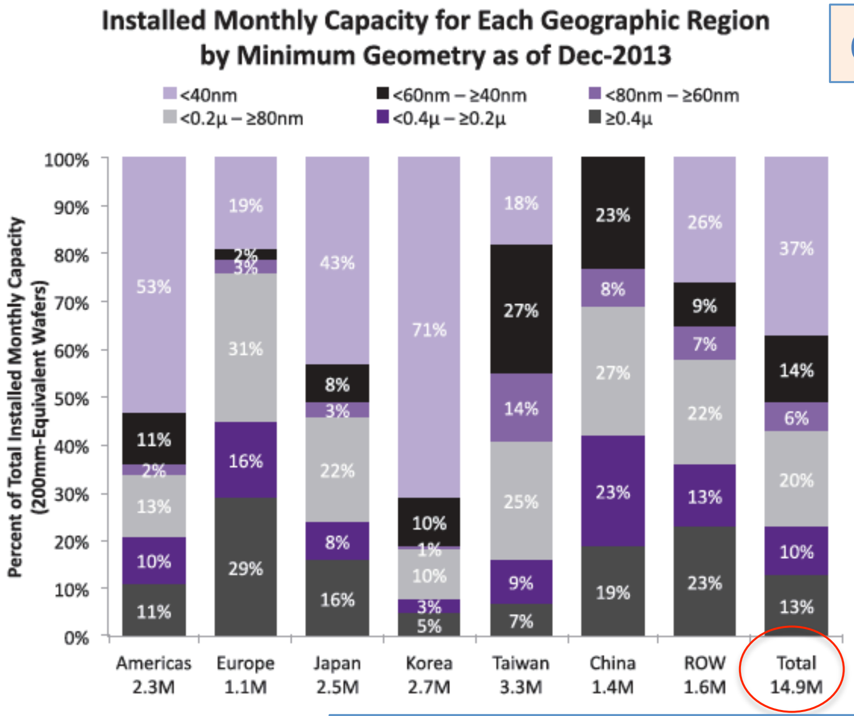

CMOS sub-micron fabs

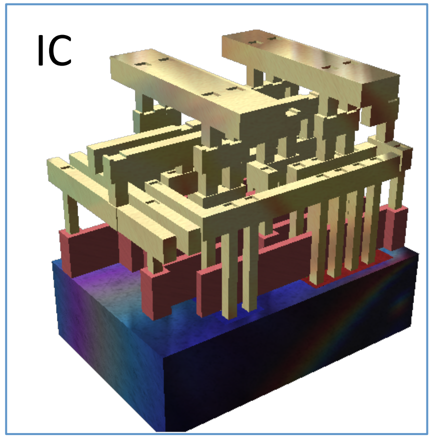

~3.5$ / cm^2

180 Million wafers / year → ~ 9 x 10^6 m^2

Silicon Properties – Lattice Structure

Silicon Atom (Si)

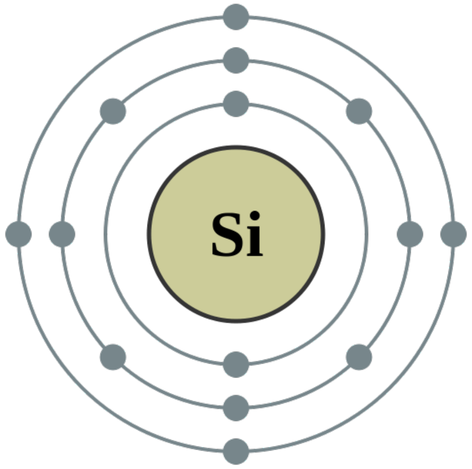

- Z = 14 (2,8,4)
- Group IV
- 4 valence electrons

2D representation of Si crystal

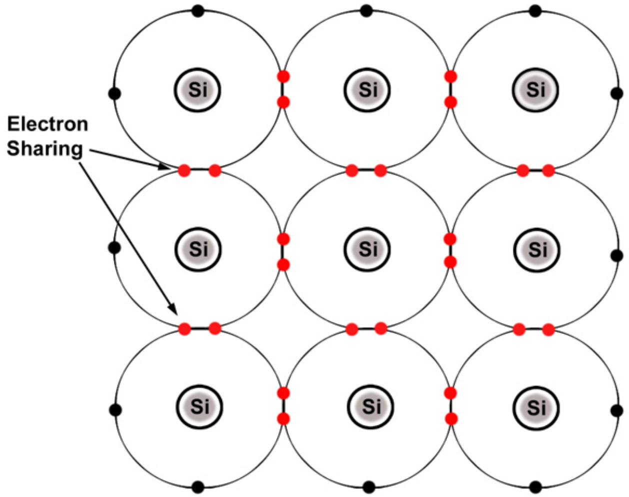

Shared electrons of a covalent bond

Silicon lattice – diamond crystal structure

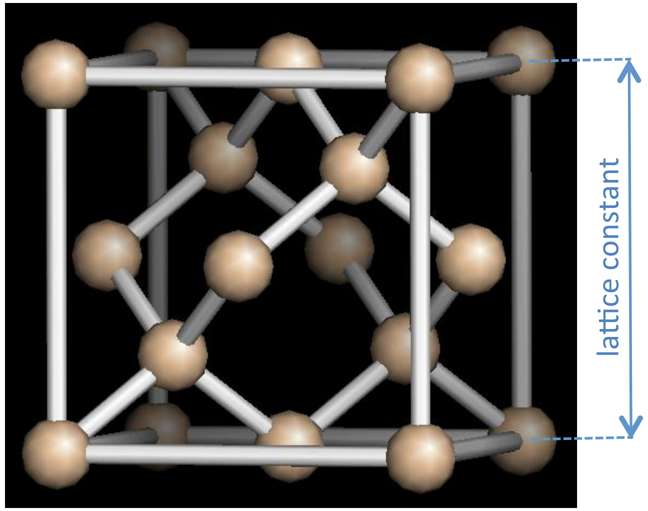

Crystal structure
- diamond cubic (tetrahedral)
- lattice constant 5.43 A

Each atom is surrounded by 4 equidistant nearest neighbors

Silicon Properties – Lattice Structure

For a single atom the electrons can only occupy certain energy levels

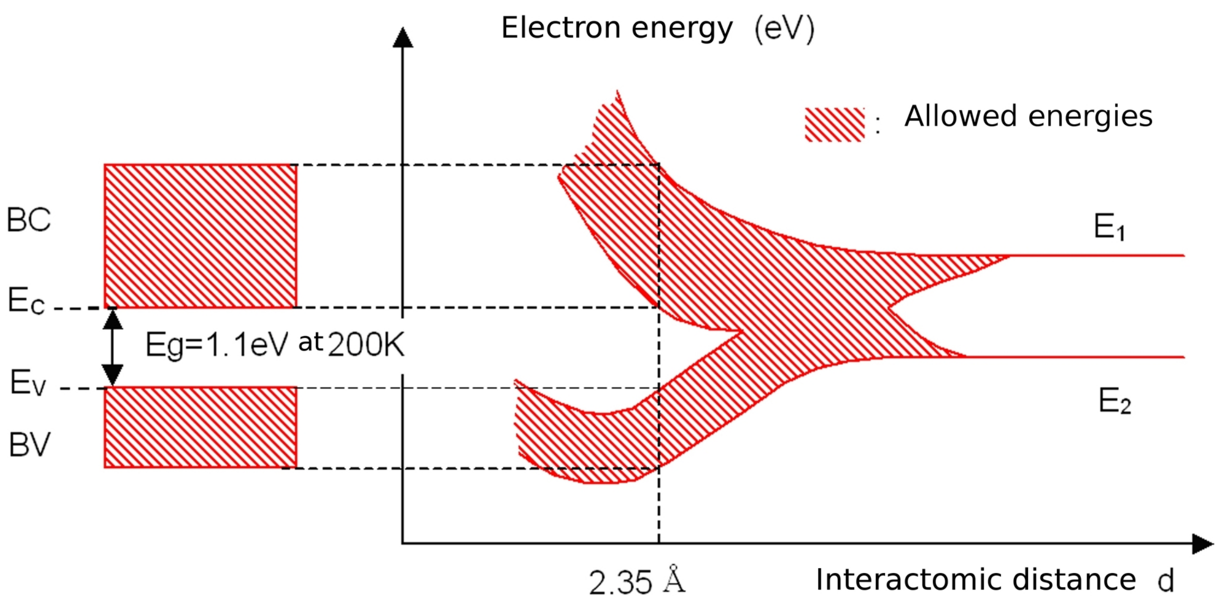

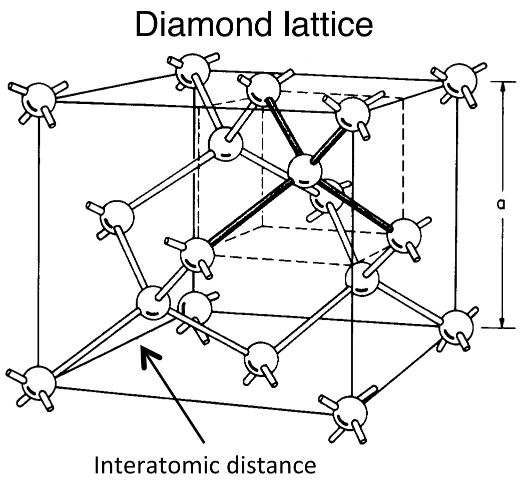

When N atoms are moved closer, until they reach the equilibrium inter-atomic distance d, the energy levels split into N levels (N-fold degenerate) very close to each other. If N is large (which is the case in a crystal) they eventually form a continuous energy band.

In a crystal the discrete atomic levels form energy bands

Material Basic Properties

Solid state materials classification

- isolators (large band gap)
- **semiconductors** (small band gap)
- metals (conduction band partially filled or overlaps with valance band)

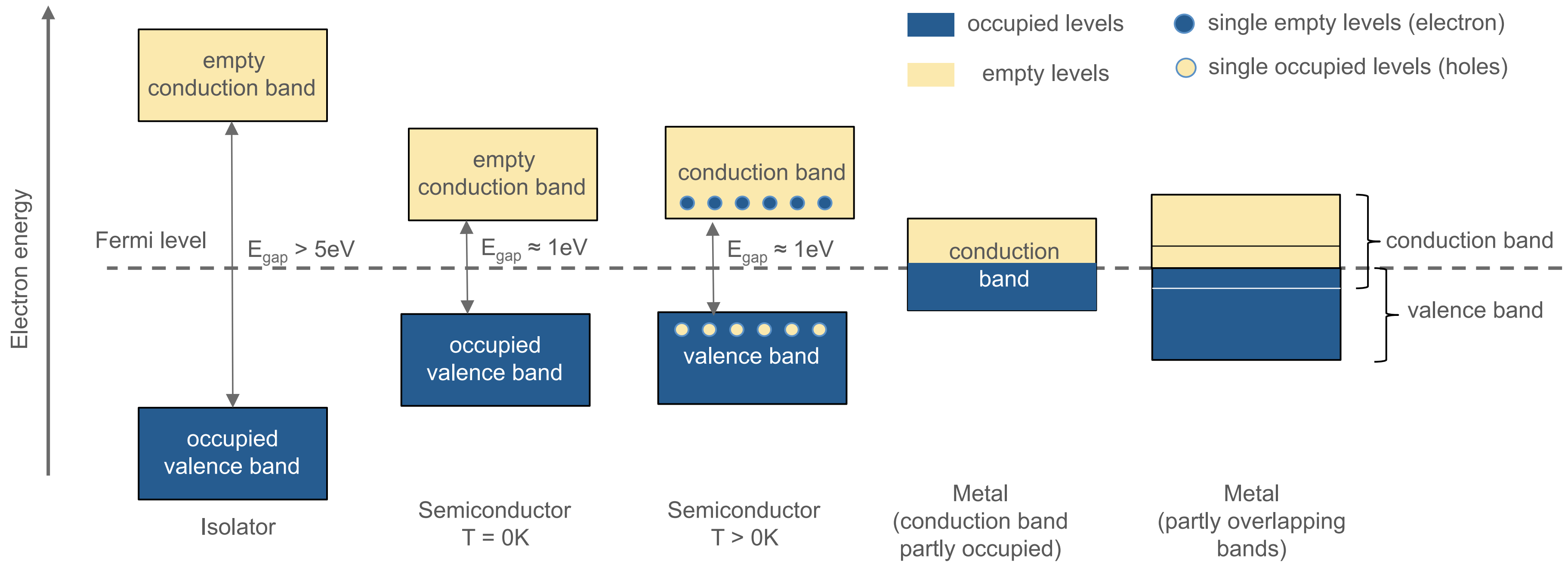

Band gap at 300K: **Si = 1.12eV**, Ge = 0.67eV, GaAs = 1.42eV, Diamond = 5.5eV

Band gap Si at 0K: 1.17eV

Note: in reality the band structure is more complex, depending on crystal momentum, crystal orientation, etc.

Semiconductor Basic Properties

At absolute zero (-273.15°C)

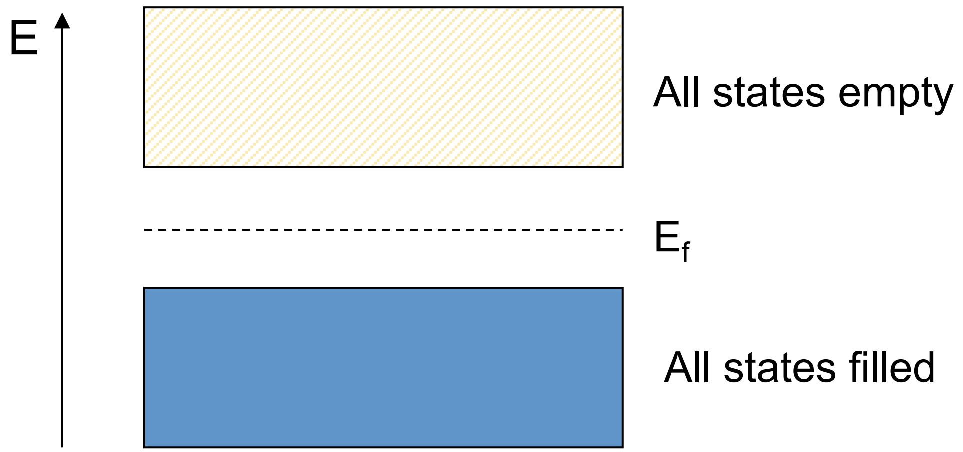

E_f … Fermi Energy

If an electrical field is applied to the crystal no current can flow as this would require an electron to acquire energy. This is not possible because no higher energy states in the valence band are available.

At higher temperatures

Electrons can gain energy due to thermal excitation

Probability that an electronic state is occupied by an electron follows the Fermi-Dirac statistics

$$F(E) = \frac{1}{1 + e^{(E - E_F)/kT}}$$

k ... Boltzmann constant

E_F is the energy at which the probability of occupation is 1/2.

$\varepsilon = E, \mu = E_f$,

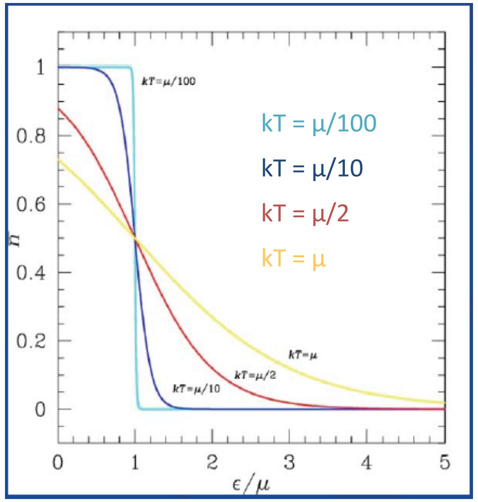

Fermi-Dirac distribution. States with energy ε below the Fermi energy (μ) have higher probability n to be occupied, and those above are less likely to be occupied.

Silicon Basic Properties

How much energy is required to generate an electron-hole pair in silicon?

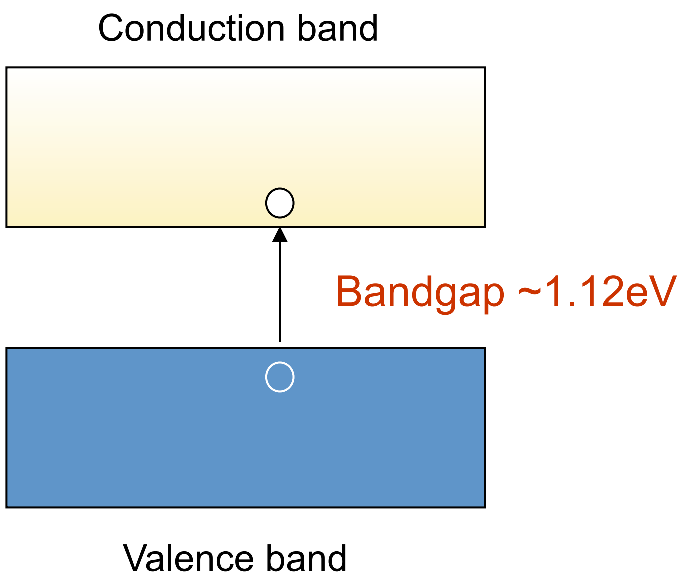

Due to phonon scattering the average energy required to generate an electron-hole pair is 3.62 eV at room temperature.

Electrons and holes

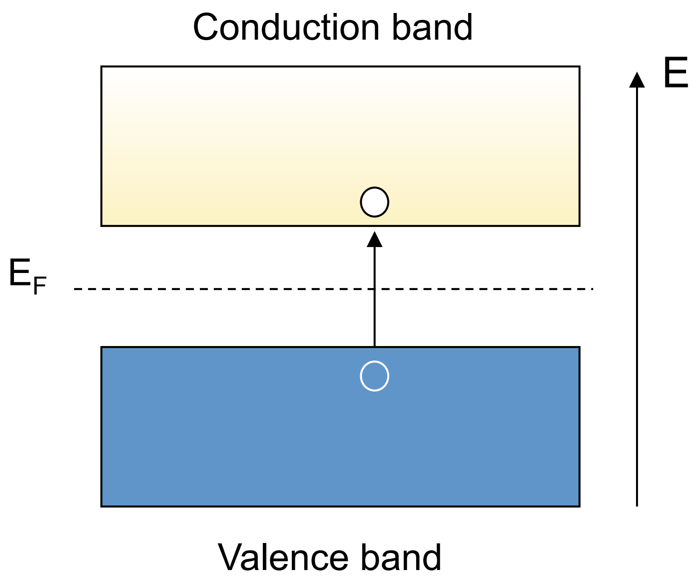

An electron moving to a state in the conduction band leaves an unoccupied state in the valence band = hole

Silicon Basic Properties

The creation of an electron-hole pair can also be seen in respect with chemical bonding: an electron is broken free from the covalent bond between two Si-atoms

Example of column IV elemental semiconductor

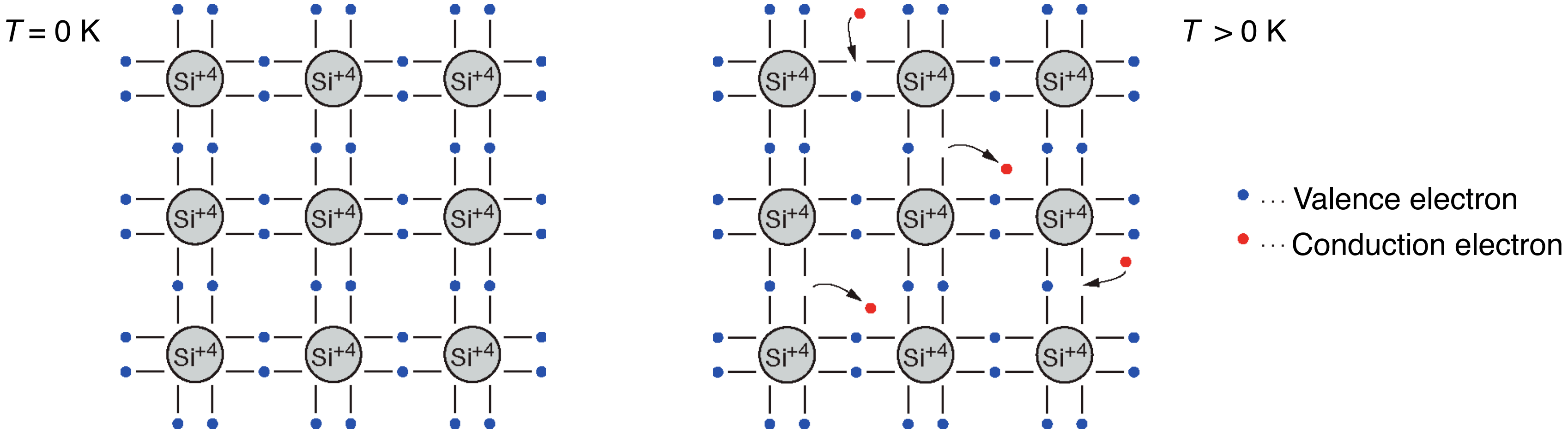

- Each atom has 4 closest neighbors, the 4 electron in the outer shell are shared and form covalent bonds
- At low temperature all electrons are bound (no conductivity)
- At higher temperature thermal vibrations of the reticle break some of the bonds ➪ free e^- cause conductivity (electron conduction)
- The remaining open bonds attract other e^- creating a vacancy (hole) ➪ The holes change position creating conductivity (hole conduction)

Silicon Basic Properties

Intrinsic semiconductor: contains only small amounts of impurities compared to the thermally generated electrons and holes

$n_e = n_p = n_i$ n_i = intrinsic carrier density

$$E_F = E_i = \frac{E_C + E_V}{2} + \frac{kT}{2}\ln\left(\frac{N_V}{N_C}\right)$$

E_F lies very close to the mid band gap at RT

N_V, N_C := effective densities of states in the valence band and conduction band

- Due to the small band gap electrons already occupy the conduction band at room temperature
- Electrons from the conduction band may recombine with holes
- A thermal equilibrium is reached between excitation and recombination: charge carrier concentration $n_e = n_h = n_i$

$$n_i = \sqrt{N_C N_V} \cdot e^{\left(-\frac{E_G}{2kT}\right)} \propto T^{\frac{3}{2}} \cdot \exp\left(-\frac{E_g}{2kT}\right)$$

N_V, N_C: effective densities of states in the valence band and conduction band

At RT: $N_V = 1.04 \times 10^{19}$ cm^{-3}, $N_C = 2.8 \times 10^{19}$ cm^{-3}

⇨ n_i (Si at RT) = 1.45×10^{10} cm^{-3}

Compared to ≈ 1×10^{22} cm^{-3} atoms in a silicon crystal only every ≈ 10^{12}th atom is ionized at RT

Silicon Properties – Drift Velocity and Mobility

Free charge carriers can be seen as free particles - they are not associated with a lattice site

- Mean kinetic energy: 3/2 kT
- Mean velocity at RT: ~ 10^{11} μm/s

The charge carriers scatter on **lattice imperfections** due to thermal vibrations, **impurity atoms** and **lattice defects**

If no electric field is applied, the average displacement due to random motion is zero

Applying an electric field **E**:

Charge carriers will be accelerated in between random collisions in the direction determined by the electric field.

Average drift velocity (*): $v_e = -\mu_e E$ μ_e electron mobility $\mu_e = \frac{e\tau_e}{m_e}$

$v_h = -\mu_h E$ μ_h hole mobility $\mu_h = \frac{e\tau_h}{m_h}$

m_e, m_h … effective mass

τ_e, τ_h: mean free time between collisions for e and h

(*) Holds for small fields E ("acceleration" is small compared to the thermal velocity).
If the electric field is high enough so that the carrier energies are larger than the thermal energies, the drift velocities become independent of the electric field.

Silicon Properties – Carrier Mobility

In the linear region of v(E) the charge carrier mobilities are

μ_e=1350 cm^2/Vs μ_h=480 cm^2/Vs

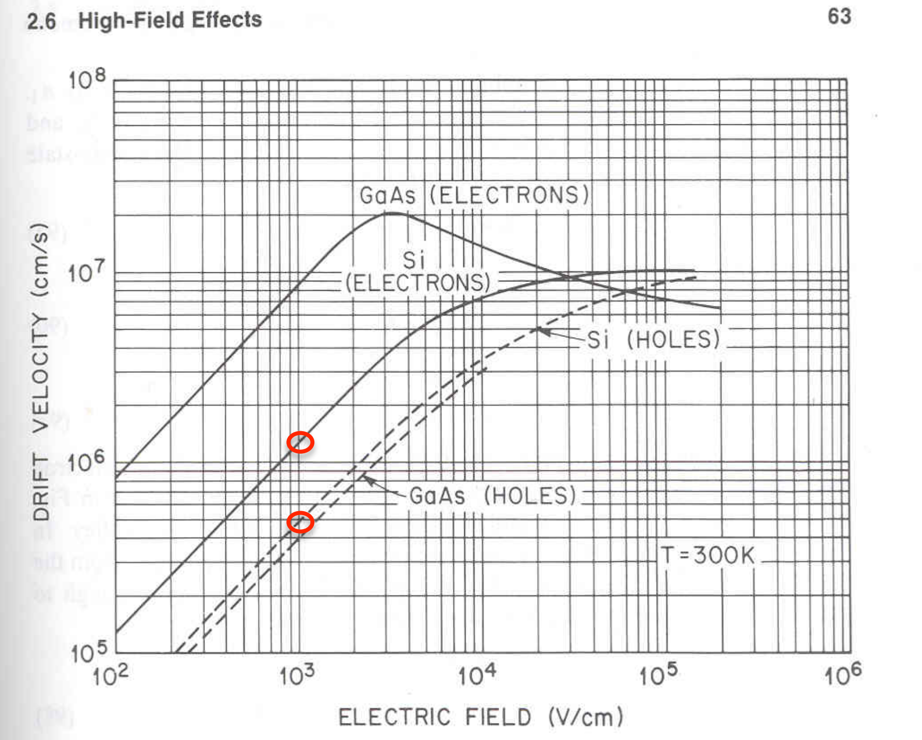

Fig. 23 Drift velocity versus electric field in GaAs and Si.[12, 13] Note that for *n*-type GaAs, there is a region of negative differential mobility.

From Sze, *Semiconductor Devices 1985*

2V is applied over 20µm

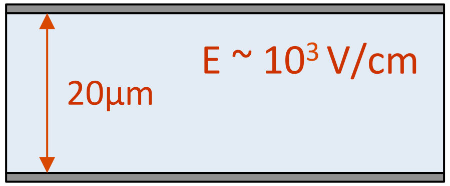

0V

$v_e \sim 10^{10}$ µm/s

$v_h \sim 0.5 \times 10^{10}$ µm/s

Charge collection time (e)

T_e = 2ns

Adding Impurities to Intrinsic Silicon – n-doping

Silicon n-type

Doping with an element of the V group (e.g. P, As, Sb). The 5th valence electron is weakly bound

- The doping atom is called donor
- The released electron can contribute to electrical conduction and leaves a positively charged ion

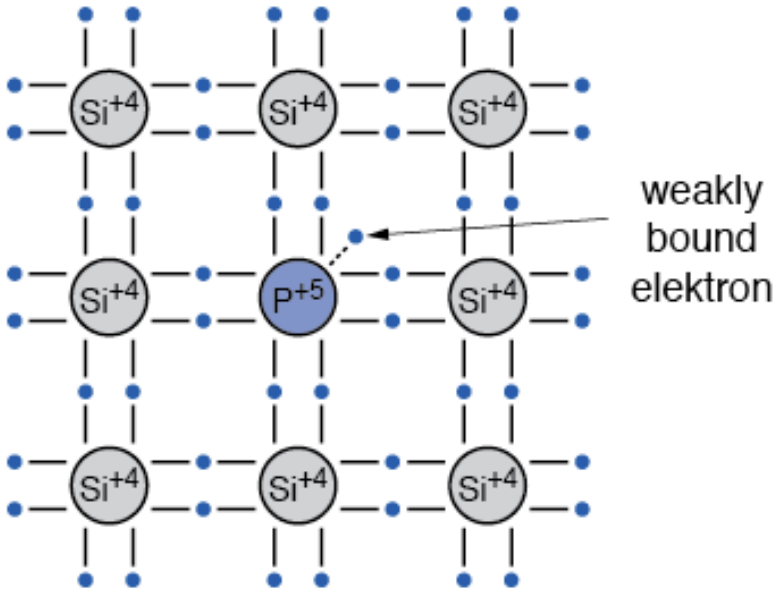

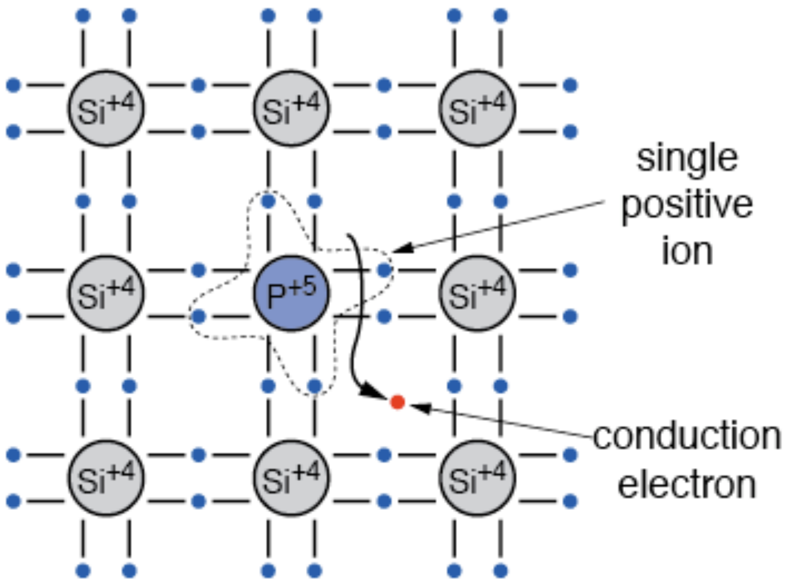

Adding Impurities to Intrinsic Silicon – Band Model n-doping

- The energy level of the donor is just below the edge of the conduction band
- At RT most electrons are raised to the conduction band
- The Fermi level E_F moves up

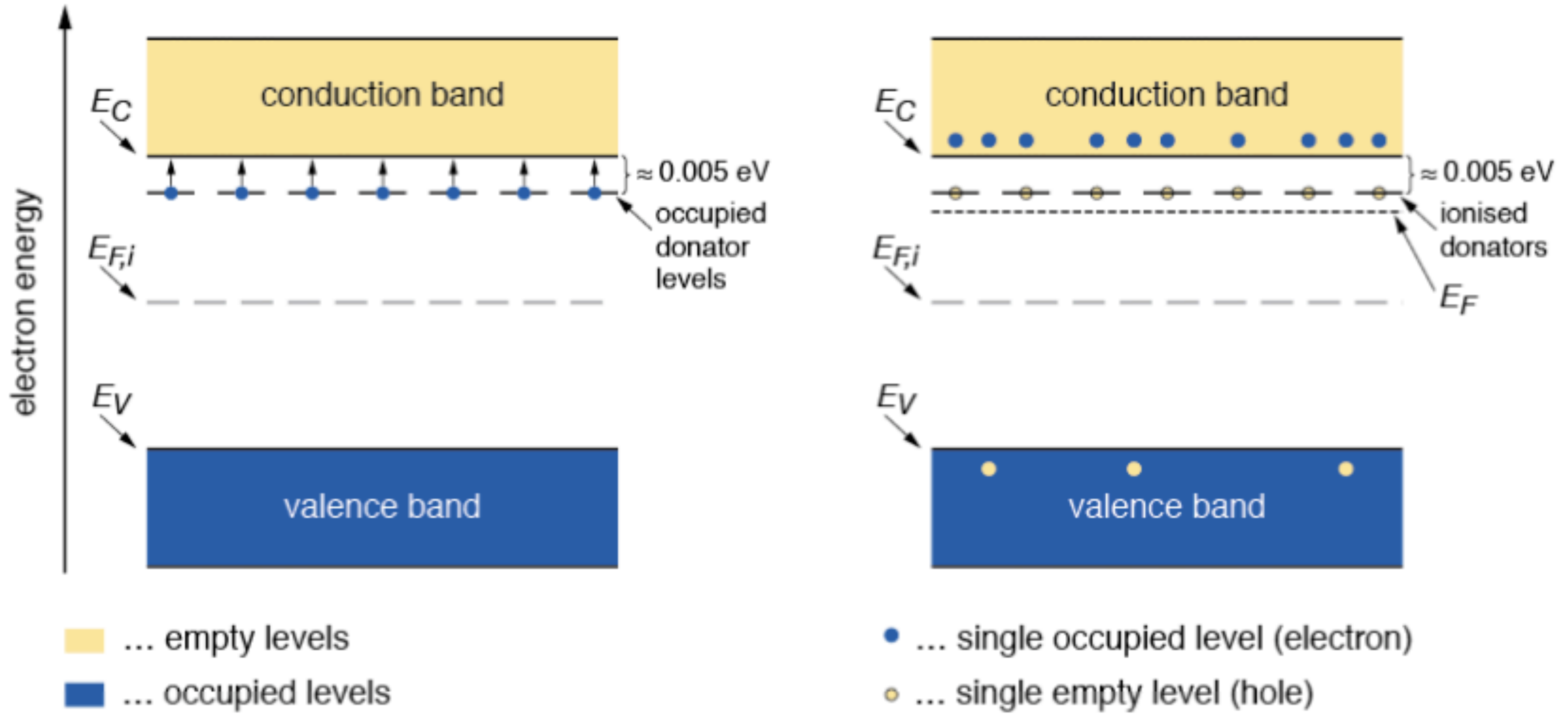

Adding Impurities to Intrinsic Silicon – p-doping

Silicon p-type

Doping with an element of the group III (e.g. B, Al, Ga, In). One valence bond remains open. This open bond attracts electrons from their neighbor atoms

- The doping atom is called acceptor
- The acceptor atom in the lattice is negatively charged. The hole acts as a free mobile charge

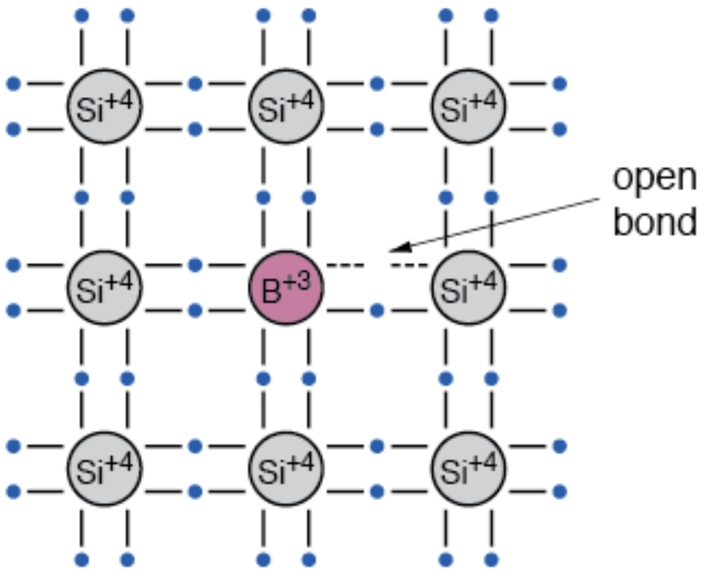

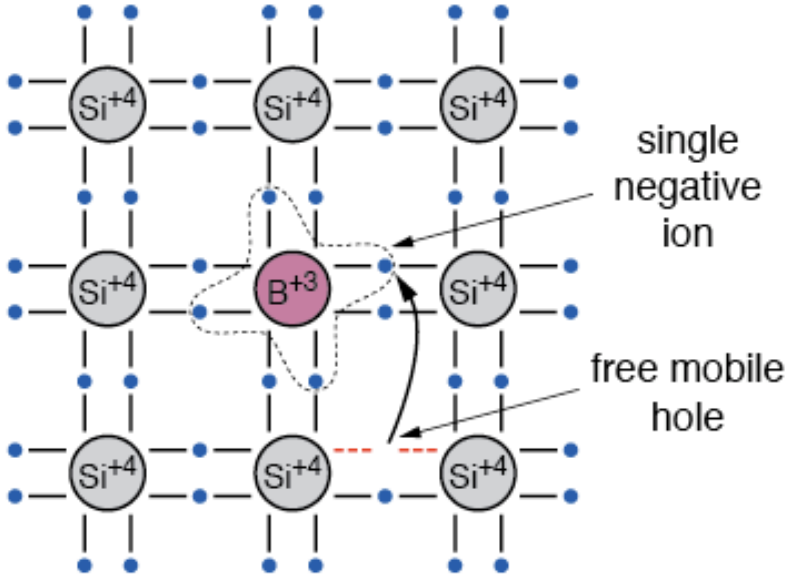

Adding Impurities to Intrinsic Silicon – Band Model p-doping

- The energy level of the acceptor is just above the edge of the valence band
- At RT most levels are occupied be electrons leaving holes in the valence band
- The Fermi level E_F moves down

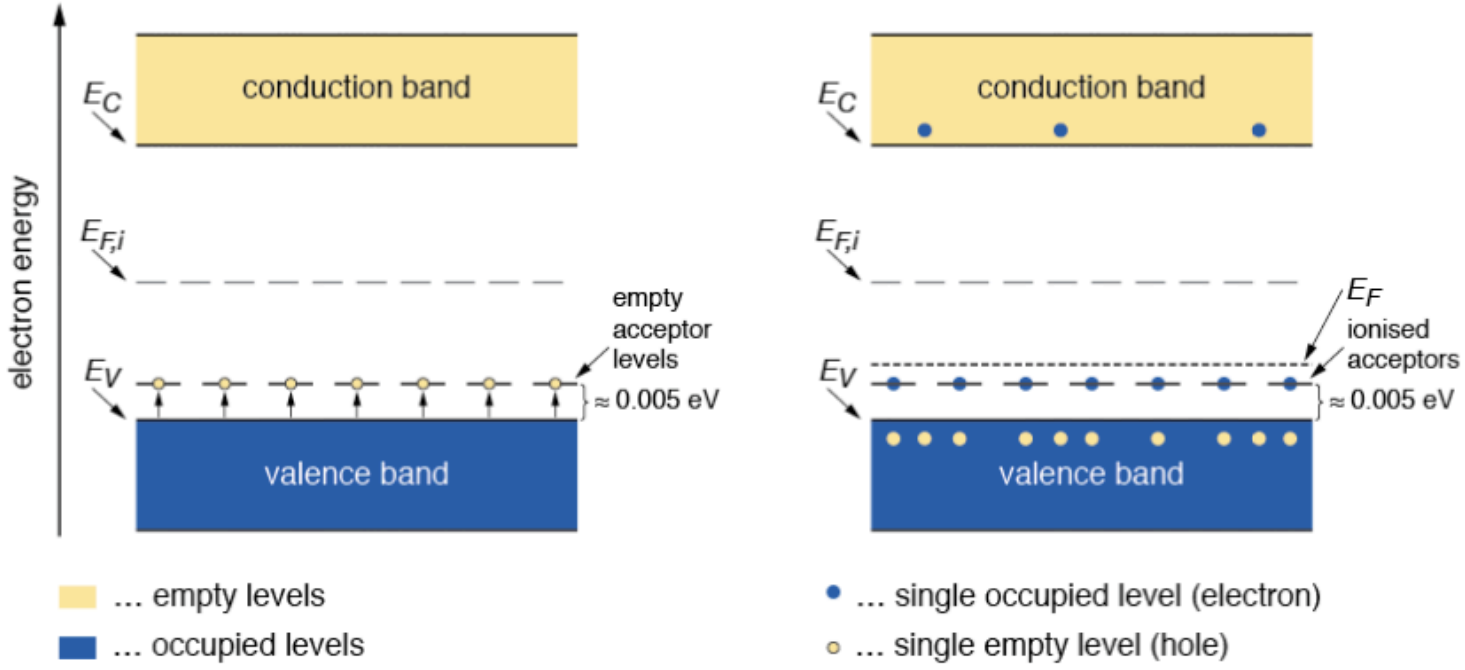

Silicon Properties – Resistivity

Depends on concentration of free charge carriers and their mobility

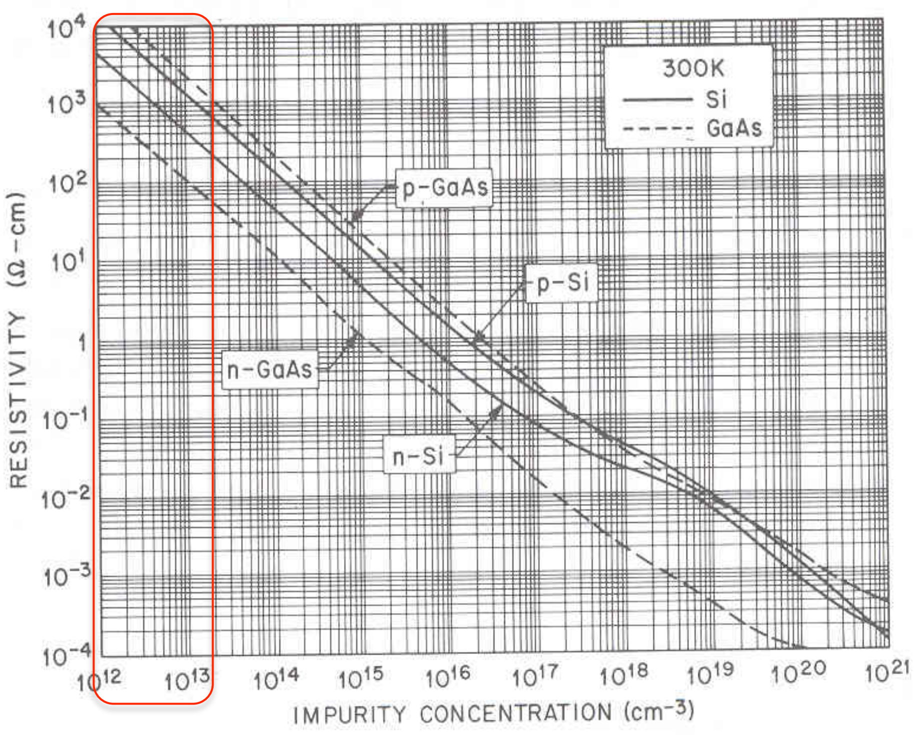

Fig. 7 Resistivity versus impurity concentration[4] for Si and GaAs.

From Sze, *Semiconductor Devices 1985*

$$\rho = \frac{1}{q(\mu_e n + \mu_h p)}$$

- ⇨ resistivity of intrinsic silicon ~ 235 kΩ cm
- ⇨ a silicon for pixel detectors ~ 1-6 kΩ cm
- ⇨ silicon substrate for CMOS IC ~ 0.1 – 10 Ωcm

Semiconductor Detectors

Basic Principles

The Ideal Semiconductor Detector

One of the most important parameters of a detector is the signal to noise ratio (SNR)

A good detector should have a large SNR. However, this leads to two contradictory requirements:

- Large Signal

  ⇨ Low ionization energy ⇨ small band gap

- Low noise

  ⇨ very few intrinsic charge carriers ⇨ large band gap

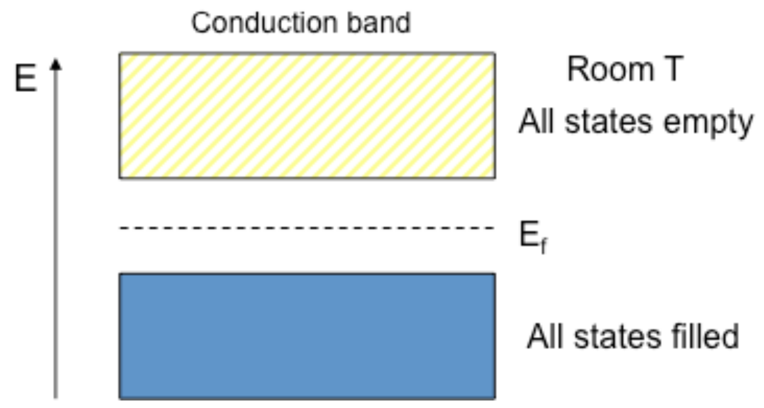

An optimal material should have $E_g \approx 6eV$

In this case the conduction band is almost empty at room temperature and the band gap is small enough to create a large number of e^-h^+ pairs by ionization.

A material with such characteristic is the diamond. However even artificial diamond (e.g. CVD diamonds) are too expensive for large area detectors.

Diamond band gap ≈ 5.5eV (RT)
Intrinsic charge carrier density
$n_i \approx 10^{-27}$ cm^{-3} (T=300K)

Intrinsic Silicon – A Very Poor Detector

How does Silicon perform as detection medium?

- Mean ionization energy $I_0 = 3.62\ eV$
- Mean energy loss for a MIP in intrinsic silicon at $T = 300\ K$: $dE/dx = 3.87\ MeV/cm$
- $n_i = 1.45 \times 10^{10}\ cm^{-3}$

Assuming a detector with a thickness of 300 μm

⇨ Signal of a MIP in such a detector

$$\frac{dE/dx \cdot d}{I_0} = \frac{3.87 \cdot 10^6\ eV/cm \cdot 0.03cm}{3.62eV} \approx \boxed{3.2 \cdot 10^4 e^- h^+}$$

Assuming a detector with a surface A = 1 cm^{-2}

⇨ Intrinsic charge carrier density (T = 300 K)

$$n_i \cdot d \cdot A = 1.45 \cdot 10^{10}\ cm^{-3} \times 0.03cm \times 1cm^{-2} \approx \boxed{4.35 \cdot 10^8 e^- h^+}$$

Number of e^-h^+ pair generated by ionization (signal) is four orders of magnitude smaller than the number of electrons generated thermally (noise) at room temeperature!!!

How to suppress the charge carriers? ⇨ Depleted zone in reverse biased pn junctions

How to Build a Detector – The p-n Junction

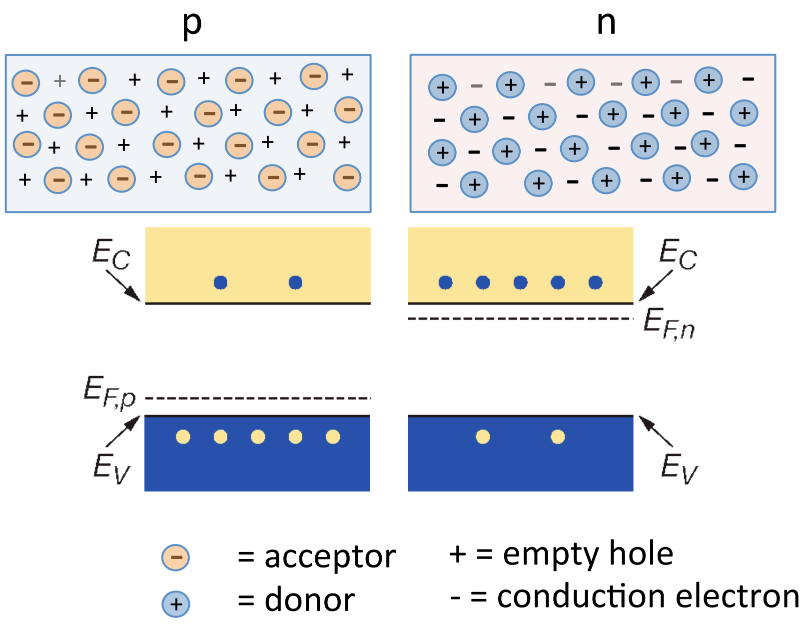

Charge carrier diffusion

At the interface of an n-type and p-type semiconductor the difference in the Fermi levels (carriers concentration) cause diffusion of the majority carriers to the other type until thermal equilibrium is reached. The Fermi levels are equal.

Opposite carriers recombine

Space charges remain in the junction region

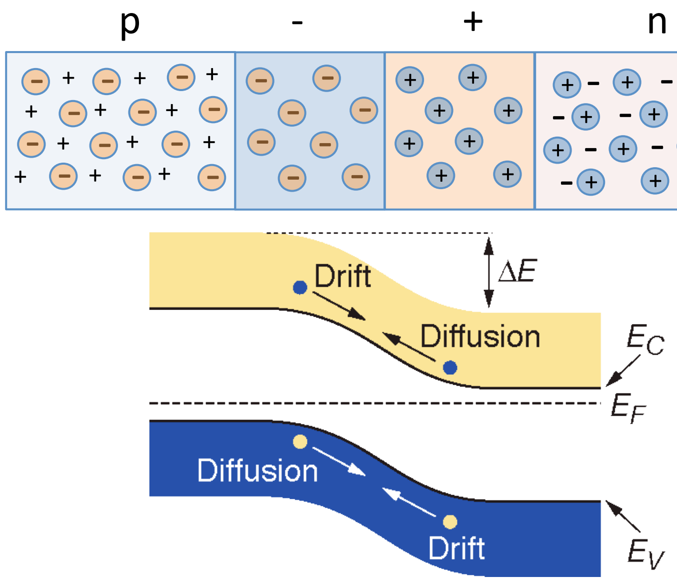

Generate an electric field, which counteract the diffusion

Depleted region, the stable charge region free of charge carriers

The corresponding potential is called built-in-voltage V_{bi}

$$V_{bi} = \frac{kT}{q} \ln \frac{N_A N_D}{n_i^2}$$

kT ~ 26 mV (at RT)

A More Realistic Detector – The p⁺n Reversed Biased Junction

Build a more Realistic Detector

Thin highly doped (**p⁺**) and **n-well** doped bulk, and apply an external voltage to deplete the bulk volume of free charge carriers

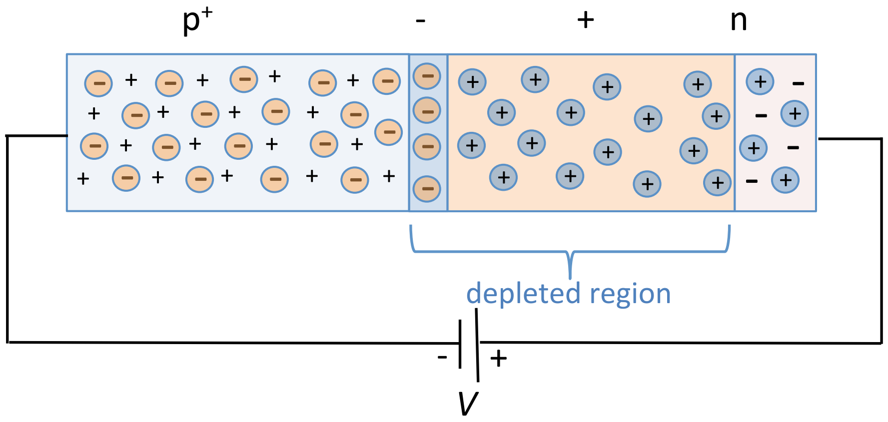

Applying a negative potential difference V between the side p and the side n (reverse bias voltage) the depleted region becomes larger

The potential barrier becomes higher by ***eV*** and diffusion across the junction is suppressed.

The current across the junction is very small ("leakage current")

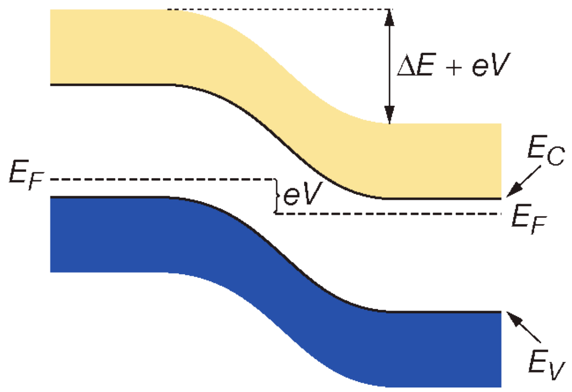

Depletion width W

$$W = \sqrt{\frac{2\varepsilon_s (V_{ext} - V_{bi})}{qN_D}}$$

ε_s = product of rel. permittivity of silicon and of vacuum

This is a reverse biased junction (diode)

A More Realistic Detector – The p^+n Reversed Biased Junction

p^+n diode detector

- Reverse bias (positive voltage on n-bulk wrt p^+ side)
- Increase reverse voltage to fully deplete the entire bulk of free charge carriers

⇨ **Full volume is sensitive to a passing particle (ionization chamber)**

- Highly n-doped layer to provide ohmic contact (n^+)

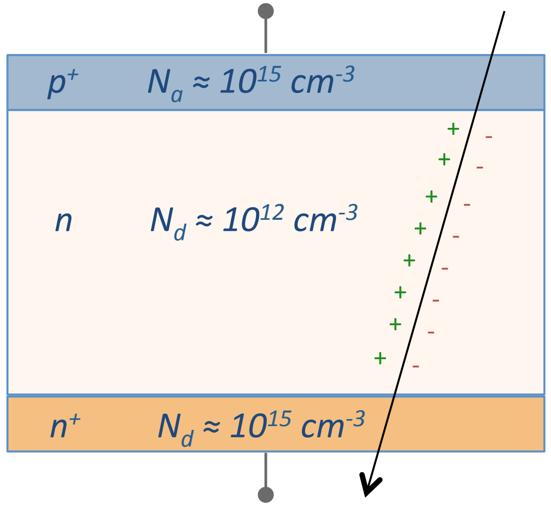

Effective doping concentrations

- $N_a = 10^{15}\ cm^{-3}$ in p^+ region
- $N_d = 10^{12}\ cm^{-3}$ in n bulk

Without applying any external voltage

- $W_p = 20$ nm, $W_n = 23\ \mu m$

Applying an external voltage of 100V

- $W_p = 400$ nm, $W_n = 363\ \mu m$

Voltage at which full thickness of the diode is depleted

$$V_{fd} = \frac{e}{2\varepsilon_s}(N_D - N_A)d^2$$

d ..thickness

N_D-N_A=N_{eff}…effective doping concentration

e.g. $N_D = 10^{12}/cm^3$, $N_a = 10^{15}/cm^3$, d = 300µm
($\varepsilon_s = 11.7 \times 8.8 \times 10^{-12}$ F/m)
V_{fd} ~ 80 V

Detector characteristics – Current-voltage (I-V)

The current-voltage characteristic curve of a p-n junction (diode): exponential increase in forward bias, small saturation in reverse bias

Ideal diode equation

$$I = I_0 \cdot \left(e^{\frac{eV_{fd}}{kT}} - 1 \right)$$

I_0 = reverse saturation current

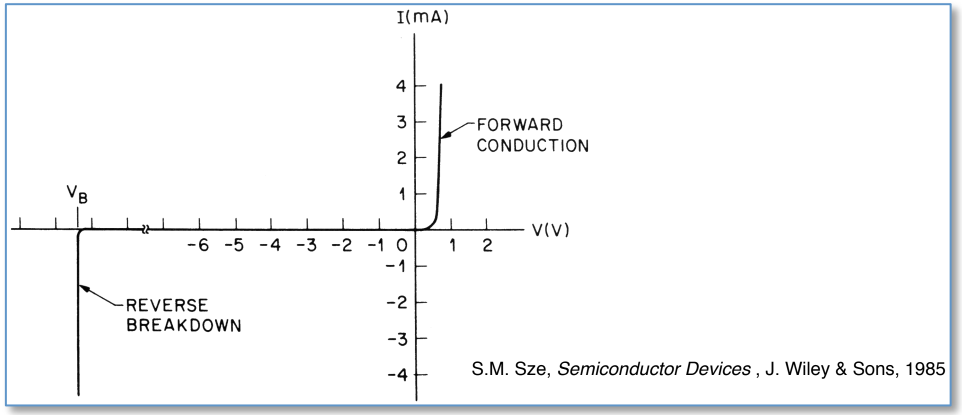

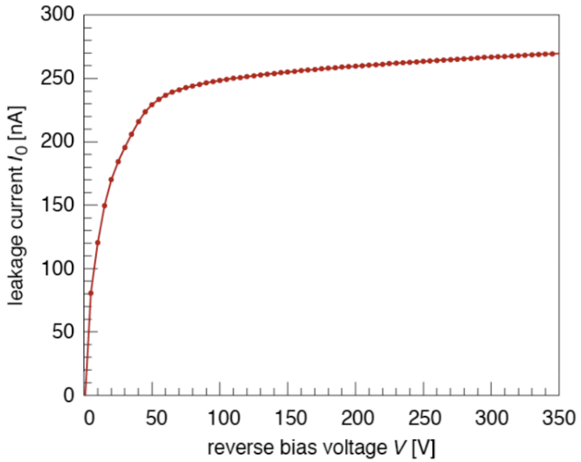

Room temperature leakage current measured on a CMS strip detector (from M. Krammer and F. Hartmann)

- A silicon detector is operated in reverse biased mode
- Reverse saturation current is relevant (leakage current)
- This current is dominated by e^-h^+ pairs generated thermally
- Due to the applied electric field they cannot recombine drift to the electrodes causing the leakage current

Detector characteristics – Depletion Voltage Capacitance

Depletion voltage = minimum voltage at which bulk is fully depleted

The operating voltage is usually chosen to be slightly higher (over depletion)

High resistivity material (i.e. low doping) requires low depletion voltage

$$V_{fd} = \frac{e}{2\varepsilon_s}(N_D - N_A)d^2$$

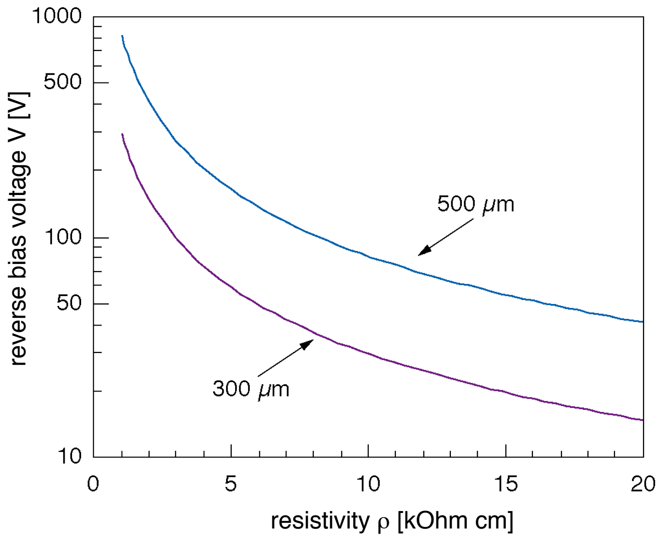

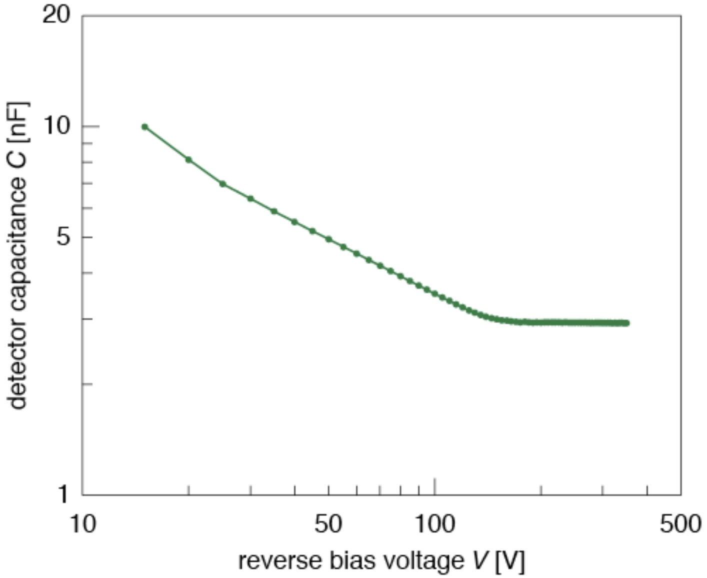

Measured detector capacitance as function of bias voltage, CMS strip detector
M. Krammer, F. Hartmann

For a Typical Si p-n junction ($N_a >> N_d >> n_i$) with planar geometry, the detector capacitance is

$$C = \sqrt{\frac{\varepsilon_0 \varepsilon_r}{2\mu\rho|V|}} \cdot A$$

ρ: resistivity of the bulk

μ: mobility of majority carrier

V: bias voltage

A: detector surface

Microstrip Detector – DC Coupled Detector

A charged particle traversing the detector generates by ionization a trail of e^-h^+ pairs ($\approx$ 100 $e^-h^+/\mu m$)

These charges drift to the electrodes (strips) inducing a current (charge moving in an electric field)

The (drift) current is amplified by an electronic circuit connected to each strip

From the signals on the individual strips the position of the particle can be reconstructed

A typical n-type Si strip detector

- p^+n junction: $N_a \approx 10^{15}$ cm^{-3}, $N_d \approx$ 1-5 10^{12} cm^{-3}
- n-type bulk: ρ > 2kΩcm
- thickness 300μm
- Operating voltage < 200V
- n^+ layer on backplane to improve ohmic contact
- Aluminum metallization

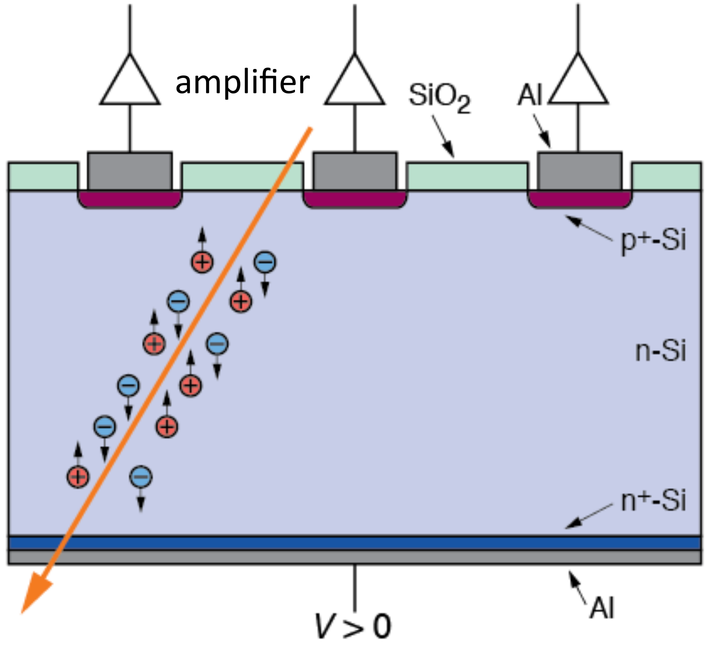

From M. Krammer and F. Hartmann (EDIT 2011)

Microstrip Detector – AC Coupled Detector

AC coupling blocks leakage current from the amplifier

- Integration of coupling in standard planar process
- Deposition of SiO_2 with a thickness of 100-200nm between p^+ and aluminum strip

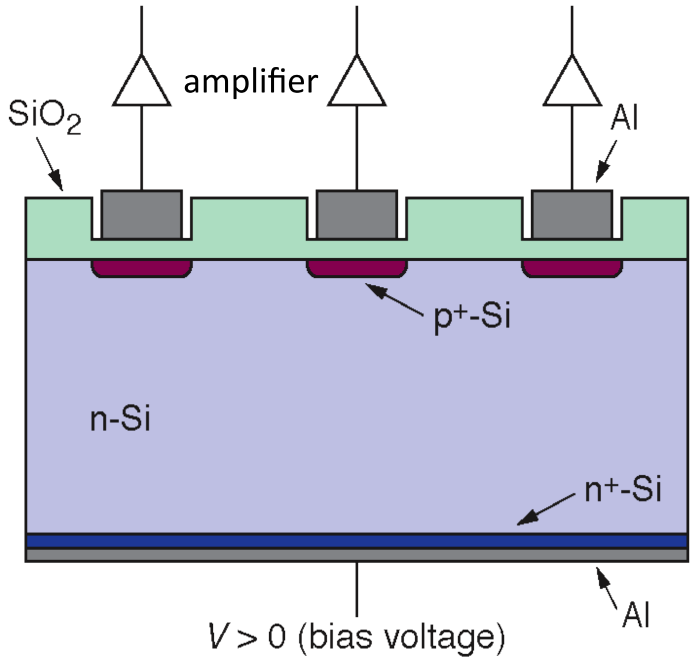

From M. Krammer and F. Hartmann (EDIT 2011)

- Depending on oxide thickness and strip width the capacitance are in the range 8-32pF/cm
- Problems are shorts trough the dielectric (pinholes) usually avoided by a second layer of Si_3N_4
- Several methods to connect the bias voltage: polysilicon resistor, punch trough bias, FOXFET bias

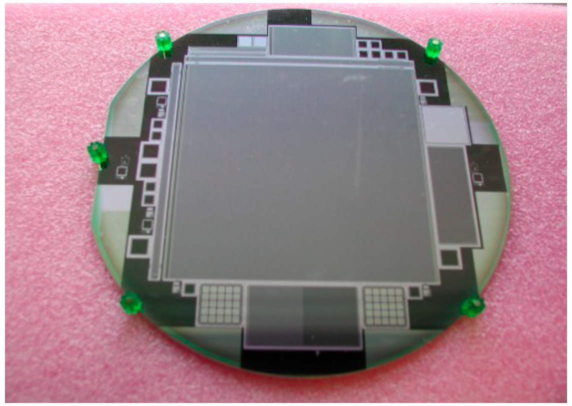

Microstrip Detector – Polysilicon Bias Resistor

- Deposition of polycristalline silicon between p^+ implants and a common bias line
- Depending on width and length a resistor of up to $R \approx 20\ M\Omega$ is achieved ($R = \times R_s \times length/width$)
- To achieve high resistor values winding poly structures are deposited
- Drawback: additional production steps and photo lithographic masks required

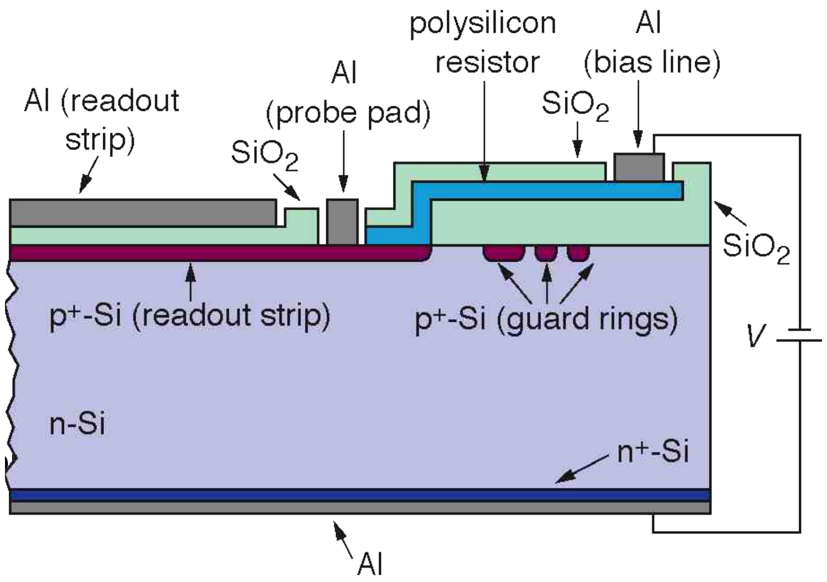

Cut through an AC coupled strip detector with integrated poly resistors

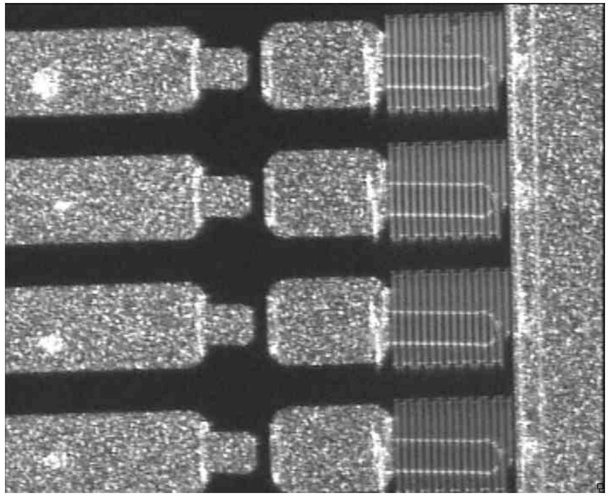

Close view of area with polysilicon resistors, probe pads, stip ends. (CMS microstrip detector)

Pixel Detectors

Hybrid Pixel Detector

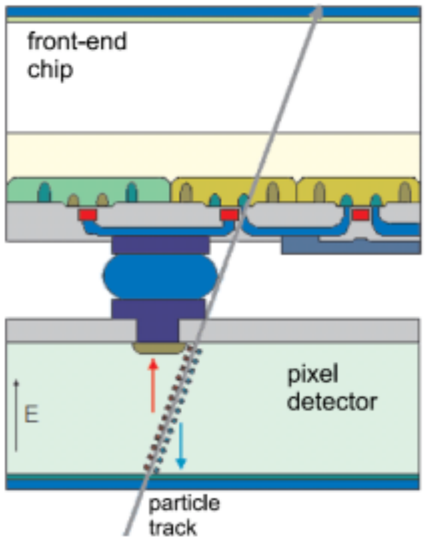

N. Wermes (Univ. of Bonn)

- Sensor based on silicon junction detectors produced in a planar process
- High resistivity wafers (few kΩcm) with diameters of 4” – 6” (8’’ now becoming available)
- Specialized producers (~10 world wide)
- Readout Chip: ASIC - CMOS sub-micron technology
- Interconnect technology based on flip-chip bonding

➔ currently installed at the LHC experiments

Monolithic Pixel Detector

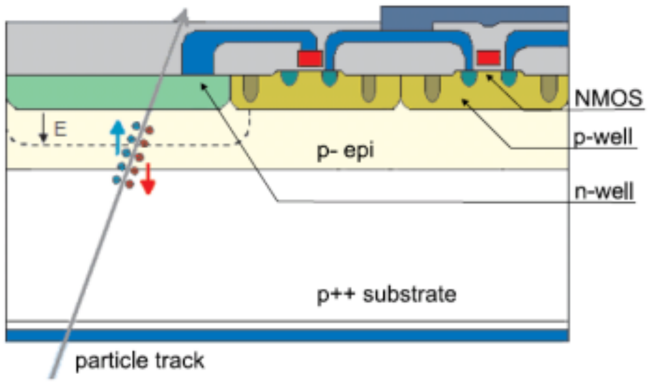

- Charge generation volume integrated into the ASIC
- Exist in many different flavours: **CMOS**, HV/HR CMOS, DEPFET, SOI, …
- The following will cover only CMOS Monolithic Active Pixel Sensors (CMOS MAPS) = CMOS Pixel Sensors (CPS)

Hybrid Pixel Detectors

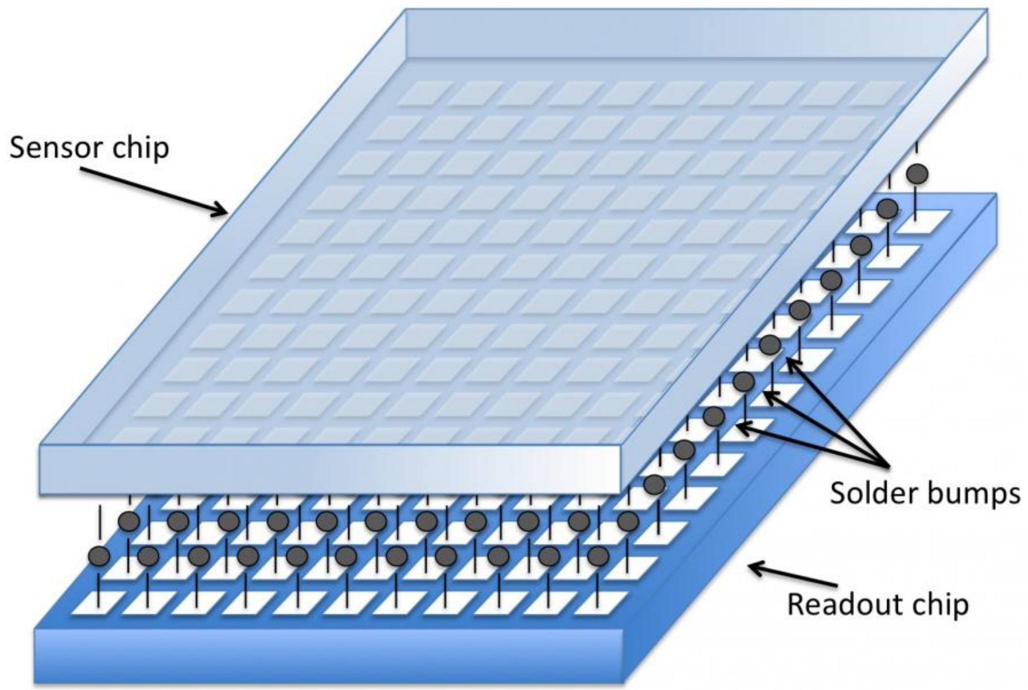

Each pixel cell in the sensor is connected to a pixel cell in the readout chip via a bump bond

Advantages

- Pixel detector provides truly space-point information (3D coordinates) removing hit ambiguities
- Small pixel area
  - Low detector capacitance (~fF)
  - Large signal-to-noise ratio (e.g. 150:1)
- Small pixel volume
  - Low leakage current (~1 pA/pixel)
- n^+-on-n for the LHC
  - Electron have faster collection time

Disadvantages

- Large number of readout channels
- Large bandwidth
- Large power consumption
- Bump bonding is costly and complex

Hybrid Pixel Detectors

1. Pixel Sensor

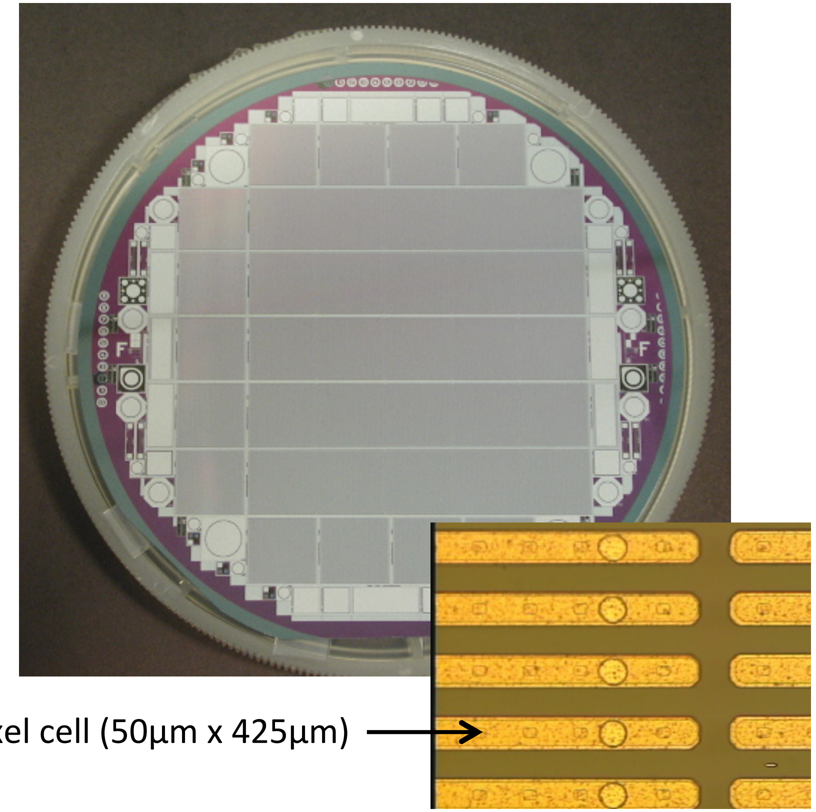

Pixel cell (50µm x 425µm)

2. Readout Chip (ASIC)

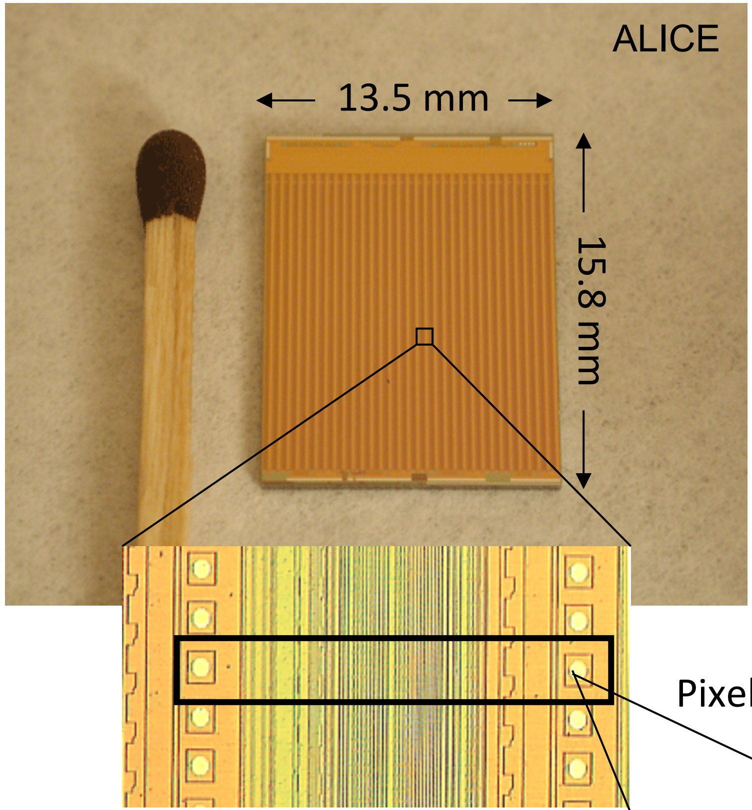

Pixel cell (e.g. 50 µm x 425 µm)

3. Bump Bond

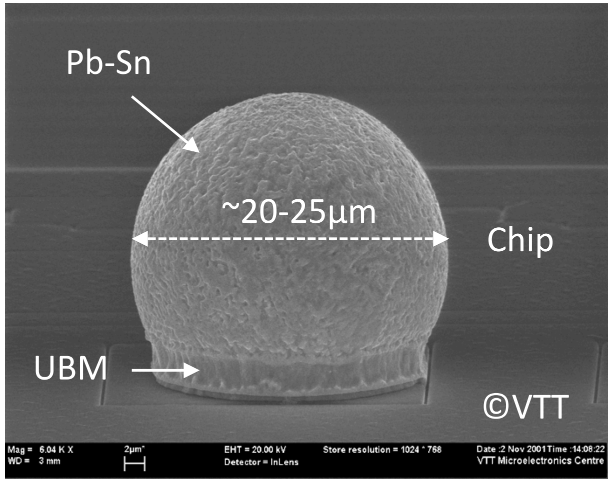

SEM picture of one bump bond

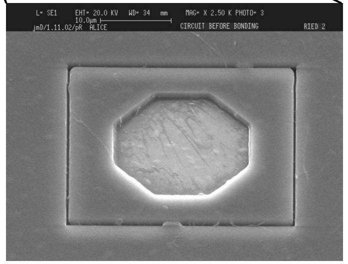

Bump bonding pad

Each pixel cell in the sensor is connected to a pixel cell in the readout chip via a bump bond

Usually several readout chips are connected to a single sensors

Hybrid Pixel Detectors

How to efficiently cover large surfaces? Ladders (modules)

- sensor size limited by wafer size and bump bonding requirements (flatness!),

  ➪ LHC experiments: ~7 cm x 2 cm
- chip size limited by CMOS lithography
- larger chip -> lower yield in production

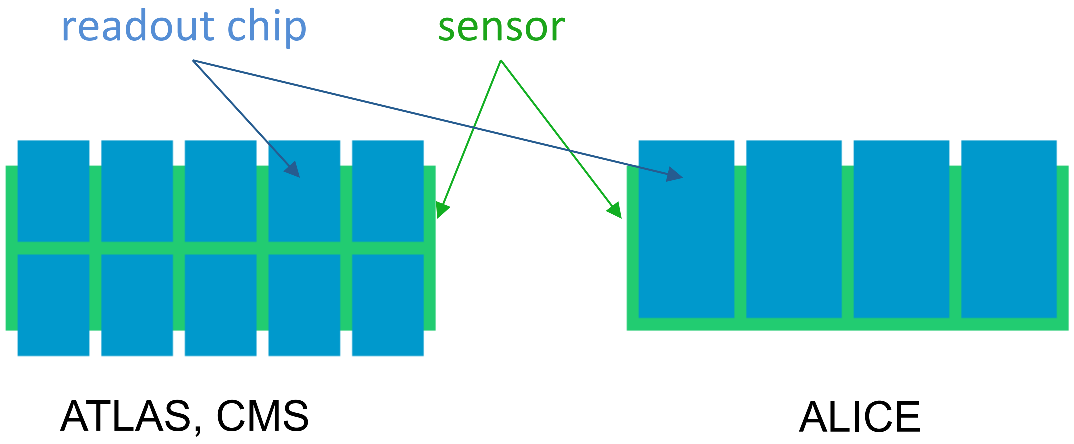

To avoid dead areas between chips: long boundary pixels

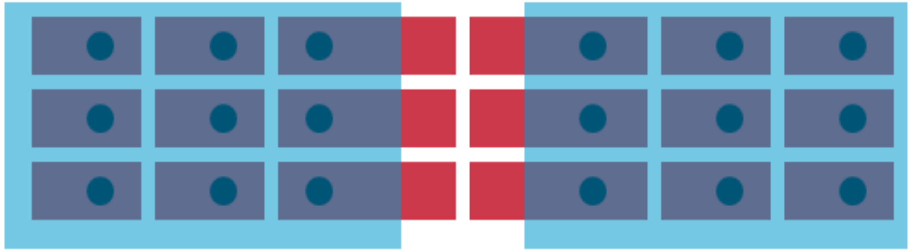

To avoid dead areas between ladders: turbine configuration ➪ higher material budget in some regions

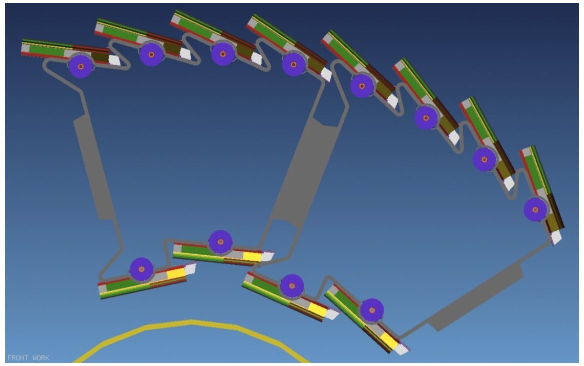

Silicon Detectors – Signal Formation

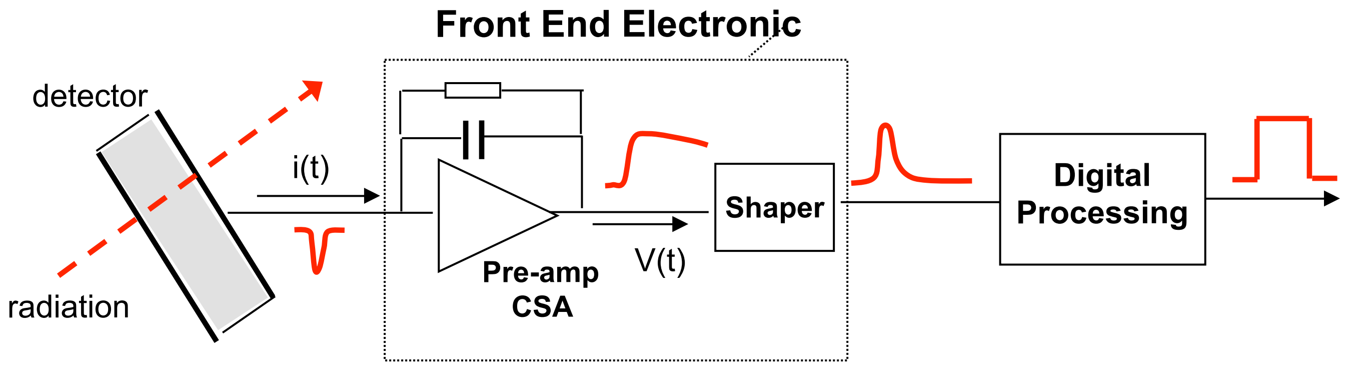

- Charge from the detector is integrated on the feedback capacitor
- The output voltage is proportional to the input charge
- V_{out} remains constant for times >t

$$V_{out} = \frac{1}{C_f}\int_0^t I_{in}(t)\,dt = \frac{Q(t)}{C_f}$$

To avoid pile-up a feed-back resistor is added in parallel to C_f to discharge C_f

References

Tracking

1. Gluckstern R.L., "Uncertainties in track momentum and direction, due to multiple scattering and measurement errors NIM 24 p. 381 (1963)"
2. Bock R. K., Grote H., Notz D., Regler M., "Data Analysis technique for high energy physics experiments", Cambridge University Press 1990
3. Blum W., Rolandi L. "Particle detection with drift chambers" Springer-Verlag1993
4. Ragusa F., "An introduction to Charged Particles Tracking, Italo-Hellenic School of Physics (2006)"
   See: http://www.le.infn.it/lhcschool/talks/Ragusa.pdf

Silicon Detectors

1. Sze S.M. "Semiconductor devices – Physics and technology"
2. Lutz G., "Semiconductor Radiation Detectors – Device Physics", Springer 1999
3. Rossi L., Fischer P., Rohe T., Wermes N., "Pixel Detectors – from fundamentals to applications"
4. Bortoletto D., "Why and how silicon detectors are becoming more and more intelligent"
5. Krammer M., "Silicon detectors" – Praktikum 2010-11
   See: "http://www.hephy.at/fileadmin/user_upload/Lehre/Unterlagen/Praktikum/Halbleiterdetektoren.pdf"